https://doi.org/10.5194/acp-2020-859
Preprint. Discussion started: 29 October 2020

Atmospheric Chemistry and Physics Discussions

ENSO Effect on Interannual Variability of Spring Aerosols over East Asia

Anbao Zhu[1,2], Haiming Xu[1,2*], Jiechun Deng[1,2], Jing Ma[1,2], Shuhui Li[1,2]

[1]Key Laboratory of Meteorological Disaster/KLME / ILCEC / CIC-FEMD, Nanjing University of Information Science & Technology, Nanjing 210044, China
[2]School of Atmospheric Sciences, Nanjing University of Information Science & Technology, Nanjing 210044, China

Correspondence to: Haiming Xu (hxu@nuist.edu.cn)

Abstract. Effects of the El Niño/Southern Oscillation (ENSO) on the interannual variability of spring aerosols over East Asia are investigated using the Modern Era Retrospective analysis for Research and Applications Version 2 (MERRA-2) reanalysis aerosol data. Results show that the ENSO has a crucial effect on the spring aerosols over the Indochina Peninsula, southern China and the ocean south of Japan. The above-normal (below-normal) aerosols are found over these regions during the El Niño (La Niña) ensuing spring. In contrast to the local aerosol diffusion in winter, the ENSO affects East Asian aerosols in the following spring mainly via modulating upstream aerosol generation and transport processes. The underlying physical mechanism is that during the El Niño (La Niña) ensuing spring, the dry (wet) air and less (more) precipitation are beneficial for the increase (reduction) of biomass burning activities over the northern Indochina Peninsula, resulting in more (less) carbonaceous aerosol emissions. On the other hand, the anomalous anticyclone (cyclone) over the western North Pacific (WNP) associated with El Niño (La Niña) enhances (weakens) the low-level southwesterly wind from the northern Indochina Peninsula to southern Japan, which transports more (less) carbonaceous aerosol downstream. Anomalous precipitation plays a role in reducing aerosols over the source region, but its washout effect over the downstream region is limited. The ENSO's impact on the ensuing spring aerosols is mainly attributed to the eastern Pacific ENSO rather than the central Pacific ENSO.

1 Introduction

East Asia, especially China, has suffered heavy air pollution from various emission sources in recent decades (e.g., Streets and Waldhoff, 2000; Chan and Yao, 2008; Tao et al., 2017). An increase in anthropogenic aerosol emission due to human activities, such as economic development and urbanization, has been considered as the primary reason for the sharp increase of the occurrence of haze pollution events (e.g., Zhang et al., 2013; An et al., 2019). Furthermore, due to their physical and chemical properties, aerosols have adverse effects on human health (e.g., Cohen et al., 2017; Lelieveld et al., 2019) and ecosystems (e.g., Yue et al., 2017; Werdell et al., 2019).

As an important component of the atmosphere, aerosols play a crucial role in climate change through aerosol-radiation interactions (i.e., the direct effect) and aerosol–cloud interactions (i.e., the indirect effect).Aerosols can directly absorb (e.g.,

https://doi.org/10.5194/acp-2020-859
Preprint. Discussion started: 29 October 2020


Atmospheric Chemistry and Physics Discussions

dust, black and brown carbon) and scatter (e.g., sulfate, nitrate and organics) solar radiation, altering the radiation budget (Forster et al., 2007; Myhre et al., 2013), while they indirectly produce changes in radiation and precipitation via modifying cloud microphysical properties and lifetime (Rosenfeld, 2000; Rosenfeld et al., 2008; Li et al., 2011). Both effects by aerosols can induce strong large-scale atmospheric circulation change (Allen et al., 2012; Shen and Ming, 2018; Deng et al., 2020) and regional climate responses (e.g., Lau et al., 2006; Zhang et al., 2007; Wang et al., 2019a). On the other hand, climate change may also act to redistribute the East Asian aerosol loading in turn. Changes in the intensity of the East Asia monsoon can directly affect the transport and lifetime of a wide variety of aerosols (Wu et al., 2016). For instance, the weakening of the East Asia winter monsoon (EAWM) has led to an increase in heavy fog-haze over eastern China during recent years (Niu et al., 2010), while the East Asia summer monsoon (EASM) is negatively correlated with aerosol concentrations over eastern China (Zhang et al., 2010a). In addition, the East Asian aerosol variation can be modulated by climate anomalies due to external forcing factors, including the Arctic sea ice (Wang et al., 2015; Zou et al., 2017), Eurasian snowpack (Yin and Wang, 2017), and sea surface temperature (SST) (e.g., Liu et al., 2013; Feng et al., 2016b; Sun et al., 2018).

As the strongest signal of interannual climate variability, the El Niño-Southern Oscillation (ENSO) can cause remarkable climate anomalies at a global scale. Thus, it may affect the East Asian aerosols through changing atmospheric circulation. Gao and Li (2015) showed that an El Niño (La Niña) event is likely to bring more (less) haze days in eastern China in winter during 1981–2010. Sun et al. (2018) also found that the weakened EAWM during El Niño events increases aerosols in eastern China, especially over northern China. However, Zhao et al. (2018) revealed that haze days over southern China tended to be less (more) frequent in the El Niño (La Niña) winters of 1960–2014, but there is no significant relationship between ENSO and winter haze days over northern and eastern China. Using station observational data, Wang et al. (2019b) compared two individual ENSO events, and found that higher fine particulate matter ($PM_{2.5}$) concentrations were observed at most northern China stations during the El Niño (2015/2016) winter but at majority of stations in southern China during the La Niña (2017/2018) winter. However, the influence of ENSO on aerosols differs among events. Results from a chemical transport model showed that the 1987/1988 El Niño event decreased the aerosols during its mature and decay spring over eastern China, whereas the El Niño event of 1997/1998 increased the aerosols over the whole lifespan over eastern China (Feng et al., 2016b). In addition, different ENSO intensity also has different effects on East Asian aerosols. Using a climate-aerosol coupled model, Yu et al. (2019) reported that the moderate El Niño events largely increase surface aerosol concentrations over eastern China, while the strong and weak events obviously decrease the aerosol loading over northern China. Since ENSO events can be further divided into two types [i.e., the Eastern Pacific (EP) El Niño and Central Pacific (CP) El Niño (or El Niño Modoki); the EP La Niña and CP La Niña], previous studies demonstrated that the impacts of CP El Niño events on the atmospheric circulation over East Asia considerably differ from those of EP El Niño events (e.g. Weng et al., 2009; Feng et al., 2011), and the same is true for aerosols (Feng et al., 2016a, 2017; Yu et al., 2019). The CP El Niño events can increase the wintertime aerosol burden over southern China more than the EP events with the similar intensity (Yu et al., 2019). The impact of different CP La Niña events on East Asian aerosols also varies. For example, Feng et al.

https://doi.org/10.5194/acp-2020-859
Preprint. Discussion started: 29 October 2020


Atmospheric Chemistry and Physics Discussions

(2017) found an anomalous dipole pattern of aerosol concentrations over eastern China (i.e., increased aerosols in the south and reduced aerosols in the north) during the mature phase of the strong ENSO event of 1998/1999, while this dipole pattern was reversed during the moderate event of 2000/2001.

Most of these studies only focused on the winter season (Gao and Li, 2015; Sun et al., 2018; Zhao et al., 2018; Yu et al., 2019), and some discrepancies exist among these results, e.g., the regions with significant aerosol changes are different between the findings of Sun et al. (2018) and Zhao et al. (2018). However, spring sees the highest aerosol optical depth (AOD) over East Asia in the annual cycle, which is related to the dust and anthropogenic emissions (Kim et al., 2007; Bao et al., 2009). Carbonaceous aerosols (CA) from South Asia (Zhang et al., 2010b) and Southeast Asia (Lin et al., 2009; Yadav et al., 2017) can be transported to East Asia during this season. However, little attention has been paid to spring. Although a few studies attempted to reveal the impacts of ENSO on ensuing spring aerosols (Feng et al., 2016a, b, 2017; Wang et al., 2019b), their use of individual ENSO events may arise uncertainties due to the lack of statistical significance based on the long-term observational data. In addition, the different impacts of the two types of ENSO on aerosols are not thoroughly investigated. Thus, it is necessary to further explore the impacts of ENSO on ensuing spring aerosols over East Asia from a climatological perspective.

This study aims to address the following questions using long-term reanalysis aerosol data: 1) what are the impacts of ENSO on the temporal and spatial distribution of ensuing spring aerosols over East Asia? And 2) what are the physical processes and relative roles of anomalous circulation and rainfall in altering ensuing spring aerosols over the region? This study differs from previous studies, in which we focus on the influence of ENSO (including its two types) on interannual variation of East Asian aerosols in spring based on the long-term observational data and on different mechanisms in winter and ensuing spring. The rest of this paper is structured as follows. The data and methodology are presented in Sect. 2. The impacts of ENSO on the ensuing spring AOD are explored in Sect. 3. In Sect. 4, we discuss the physical mechanisms involved. In Sect. 5, we outline different influences by the two types of ENSO. In Sect. 6, we provide the discussion and conclusions.

2 Data and methods

2.1 Data and methods

We use the monthly data for atmospheric variables from the fifth generation European Centre for Medium-Range Weather Forecasts (ECMWF) reanalysis data (ERA5) (Hersbach and Dee, 2016), including geopotential height, zonal and meridional wind components on 0.25 ° grid. Monthly precipitation data on 2.5 ° grid is the Climate Prediction Center (CPC) Merged Analysis of Precipitation (CMAP) dataset (Xie and Arkin, 1997) provided by the National Oceanic and Atmospheric Administration (NOAA). We also use monthly mean SST on 1 ° grid from the HadISST V1.1 SST dataset (Rayner et al., 2003) provided by the UK Met Office Hadley Centre.

The aerosol data are the National Aeronautics and Space Administration (NASA)'s Modern Era Retrospective analysis for Research and Applications, Version 2 (MERRA-2) (Gelaro et al., 2017), with a spatial resolution of 0. 5 ° by 0.625 °

https://doi.org/10.5194/acp-2020-859
Preprint. Discussion started: 29 October 2020


Atmospheric Chemistry and Physics Discussions

(longitude by latitude) on 72 vertical levels. The MERRA-2 is generated using the advanced global data assimilation system, the Goddard Earth Observing System Model Version 5 (GEOS-5), including the assimilation of AOD retrieved from the Advanced Very High Resolution Radiometer (AVHRR) instrument over the oceans (Heidinger et al., 2014), Moderate resolution Imaging Spectroradiometer (MODIS) (Levy et al., 2010), non-bias-corrected AOD retrieved from the MISR (Kahn et al., 2005) over bright surfaces, and ground-based AERONET observations (Holben et al., 1998). This dataset includes all the processes of aerosol transport, deposition, microphysics, and radiative forcing. As the first long-term aerosol reanalysis data set, the MERRA-2 has been adequately evaluated in previous studies (e.g., Buchard et al., 2017; Song et al., 2018; Che et al., 2019; Sun et al., 2019), and widely used for analyzing the interactions between aerosols and climate systems (e.g., Lau et al., 2018; Sun et al., 2018; Che et al., 2019; Yuan et al., 2019). In this study, the monthly mean AOD at 550 nm is used to analyze the spatiotemporal characteristics of aerosols. As the tracers, aerosol species [black carbon (BC) and organic carbon (OC)] fields are used for diagnosing transport properties (Lau et al., 2018; Yuan et al., 2019).

For consistency, all of the variables cover the same period of 1980–2019. To highlight interannual variability, the Fourier analysis is performed to remove the first four waves of these variables, which are usually related to interdecadal variability (Awan and Bae, 2016). The Empirical orthogonal function (EOF) analysis, linear regression analysis, composite analysis and correlation are also used in this study and are subjected to the two-tailed Student's *t* test for statistical significance.

2.2 Identification of ENSO events

We select the ENSO events defined by the CPC. Events are defined as five consecutive overlapping 3-month periods at or above the +0.5 ℃ anomaly in the Niño 3.4 region (120 °–170 °W, 5 °S–5 °N) for warm (El Niño) events and at or below the -0.5 ℃ anomaly for cold (La Niña) events. For consecutive ENSO years, the relatively stronger El Niño and La Niña winters are taken as a representative in this study, such as 1986/87 for the 1986–1988 El Niño event, and 1999/2000 for the 1998–2001 La Niña event. Thus, 11 El Niño events (1982/83, 1986/87, 1991/92, 1994/95, 1997/98, 2002/03, 2004/05, 2006/07, 2009/10,2015/16, and 2018/19) and 12 La Niña events (1983/84, 1984/85, 1988/89, 1995/96, 1999/2000, 2005/06, 2007/08, 2008/09, 2010/11, 2011/12, 2016/17, and 2017/18) are selected.

There are many ways to distinguish the two types of ENSO events (e.g., Ashok et al., 2007; Ren and Jin, 2011). Here, following the studies of Zhang et al. (2011) and Li et al. (2019), different ENSO types are identified based on their spatial distributions of SST anomalies. When the SST anomaly centre is located east of 150 °W, the ENSO event is categorized as an EP ENSO event, in contrast to the CP ENSO event when SST anomaly centre is located west of 150 °W. This method has a distinct advantage that can effectively distinguish the two ENSO types for both El Niño and La Niña events. Then, the 11 El Niño events are divided into six EP and five CP El Niño events, and the 12 La Niña events are divided to six EP and CP types each (Table 1). A more detailed description on how to define the two ENSO types can be found in Li et al. (2019).

https://doi.org/10.5194/acp-2020-859
Preprint. Discussion started: 29 October 2020


Atmospheric Chemistry and Physics Discussions

3 Influences of ENSO on East Asian aerosols

3.1 Variation of spring aerosols

Figure 1 shows the climatological spring mean AOD in East Asia during 1980–2019. The large AOD appears over eastern China, especially over the Sichuan Basin and central-eastern China, with a maximum exceeding 0.6. The aerosol loading gradually decreases from eastern China through Japan up to the North Pacific along midlatitude westerlies, similar to the climatological annual mean AOD (Bao et al., 2009). As spring is a transitional season, relatively weak northwesterlies prevail at the low-level troposphere (850 hPa) over northern East Asia, while southern China and the north of the Indochina Peninsula are mainly controlled by the southwesterly wind, where the AOD is also relatively high. The characteristics of the spring mean AOD pattern agree well with the results of Che et al. (2019) which also used the MERRA-2 AOD in the same period.

To clarify the spatio-temporal variation of aerosols, the EOF analysis is applied to AOD anomalies relative to the 1980–2019 mean. The first EOF mode (EOF1; Fig. 2) explains 56.03% of the total variance. The spatial pattern (Fig. 2a) is highly in line with the distribution of the AOD variance (Fig. 1), characterized by large variances over the Sichuan Basin, southern China, and the Indochina Peninsula, with the maximum centre located in the northern Indochina Peninsula. Thus, an AOD index (AODI) is defined using the AOD averaged over the selected key region of (95 °–130 °E, 10 °–35 °N; the black box in Fig. 2a) with larger AOD variance. Figure 2b illustrates the respective principal component of EOF1 (PC1), together with the AODI and its interdecadal (AODI_ID) and interannual (AODI_IA) components. The correlation between AODI and PC1 exceeds 0.96, indicating that the AODI can well measure both interannual and interdecadal variation of the spring aerosol over East Asia. On the interdecadal timescale, the AODI stayed at a low level from 1980 to 1998 and increased dramatically during 1998–2013. This interdecadal change is suggested to be dominated by meteorological factors (Che et al., 2019), rather than generated by rapid economic growth as previously thought (Wu et al., 2016). However, the AODI declined rapidly after 2013, consistent with the recent study by Zhang et al. (2018), showing that the AOD over the South China had a decreasing trend since 2012 based on the MODIS records. Note that the AODI reached two peaks in early 1980s and 1990s, which were most likely associated with two giant volcano eruption events, respectively (Che et al., 2019). On the other hand, the AODI also exhibits large interannual fluctuation. Given that interannual variability is an important part of the total aerosol variability, we mainly focus on the atmospheric anomalies associated with the interannual AOD variation over East Asia in this study. Note that the variables used hereafter all refer to their interannual components.

3.2 Interannual relationships between the AOD and ENSO

Figure 3 shows the regressed anomalies of SST and near-surface (10-m) wind upon the AODI_IA during the preceding autumn [SON(-1)] and winter [D(-1)JF(0)] and simultaneous spring [MAM(0)]. During MAM(0) (Fig. 3c), anomalous SST exhibits a dipole structure in the tropical Pacific, with warmer anomalies in the central and eastern equatorial Pacific and colder anomalies in the western equatorial Pacific. Correspondingly, anomalous anticyclonic winds exist over the Northwest

https://doi.org/10.5194/acp-2020-859
Preprint. Discussion started: 29 October 2020


Atmospheric Chemistry and Physics Discussions

Pacific (NWP) and westerly anomaly winds over the central and eastern equatorial Pacific. In the Indian Ocean, warmer SST anomalies can be observed almost across the whole basin, with anomalous northeasterly winds to the north of the equator and anomalous northwesterly winds to the south. This El Niño-like SST anomaly pattern suggests that the East Asian aerosols in spring may be modulated by the preceding ENSO. Furthermore, these typical El Niño features can be found during the preceding autumn (Fig. 3a) and winter (Fig. 3b). The correlation of AODI_IA with Niño 3.4 SST reaches the maximum in the pre-winter (pre-autumn: 0.53, pre-winter: 0.6, spring: 0.58, and all of them are statistically significant at the 95% level). Thus, these coherent correlations clearly indicate that the interannual variation of East Asian aerosols is significantly correlated with the ENSO, i.e., the warm phase of ENSO (i.e., El Niño) is associated with higher aerosol concentrations in the following spring over East Asia, while the cold phase (i.e., La Niña) correlates to lower aerosol concentrations.

To further demonstrate the influence of ENSO on East Asian aerosol concentrations, the composite anomalies of the ensuing spring AOD of El Niño, La Niña events and their differences (El Niño minus La Niña) are shown in Fig. 4. During the El Niño events (Fig. 4a), positive AOD anomalies are seen over southern China, the Indochina Peninsula and equatorial Maritime Continent, which maximize in the northern Indochina Peninsula with a value of approximately 0.1, accounting for about 20% of the climatological AOD mean (Fig. 1), while the La Niña events see the opposite (Fig. 4b), especially in the northern Indochina with the largest negative anomaly around −0.08 (accounting for ~ 13% of the climatological mean). Meanwhile, prominent positive AOD anomalies are observed over parts of northwestern China and northeastern Asia. This may be due to the deserts in northwestern (Taklimakan Desert) and central (Badain Juran Desert) China, which provide more dust aerosols in the troposphere in the ensuing spring of La Niña events (Gong et al., 2006). Significant positive AOD anomalies are also found over the Indo-Gangetic Plain and parts of the northern Indian Ocean, as more dust aerosols can be transported to these regions from the deserts of Middle East, West Asia and northwestern India during April–May of La Niña years (Kim et al., 2016). Generally, the amplitude of AOD anomalies during La Niña events is much smaller than that during El Niño events, suggesting that there is an asymmetry in the effects of ENSO on aerosols over East Asia during the ensuing spring. The asymmetric influences of the ENSO on East Asian aerosols can also be found in winter, as reported (Sun et al., 2018; Feng et al., 2019). The differences between El Niño and La Niña events exhibit pronounced positive AOD anomalies covering areas from south of Japan (135 °E, 30 °N) through southern China and Indochina Peninsula to the coast of Sumatra (Fig. 4c). Note that Wu et al. (2013) pointed out aerosols increased sharply over the Maritime Continent in the fall of El Niño-developing years during the period 2000–2010, while our results indicate that positive AOD anomalies can also be observed over the Maritime Continent during the spring following El Niño.

In summary, the ENSO can significantly increase (decrease) the ensuing spring aerosol loading over the Indochina Peninsula, southern China and the downstream regions during its warm (cold) phase, and an asymmetry exists between these two phases. However, Sun et al. (2018) found that ENSO exerts a significant influence on winter aerosols over northern China, while there is no significant signal over southern China. Clearly, different mechanisms may work for the different impacts of

https://doi.org/10.5194/acp-2020-859
Preprint. Discussion started: 29 October 2020


Atmospheric Chemistry and Physics Discussions

ENSO on aerosols in winter and ensuing spring. In the following section, we will explore possible mechanism through which the ENSO can impact the ensuing spring aerosols.

4 Possible mechanisms for ENSO impacts on the East Asian aerosols

Large-sale atmospheric circulation and precipitation play crucial roles in the transport, diffusion and removal of aerosols (e.g., Bao et al., 2009; Zhang et al., 2010a; Ning et al., 2018; Feng et al., 2019). Thus, to identify the underlying mechanism associated with the effects of ENSO on the ensuing spring aerosols over East Asia, we show composite anomalies of SST, 850-hPa wind and precipitation in the spring following ENSO events (Fig. 5). For the spring following the El Niño event (Fig. 5a), tropical Pacific SST anomalies (SSTAs) generally display a zonal dipole structure with warm anomalies in the eastern-central equatorial Pacific and cold anomalies in the western equatorial Pacific. Note that some cold anomalies can also be seen on both sides of the warm anomalies. Meanwhile, a strong anomalous surface high pressure is located over the NWP (not shown), which is centred over the Philippine Sea. Thus, the anomalous anticyclone (AAC) over the NWP acts to bridge the eastern-central Pacific warming and East Asian climate (Harrison and Larkin, 1996; Wang et al., 2000). On the southeast flank of the NWP AAC, the anomalous wind there intensifies the prevailing northeasterly wind, which contributes to the SST cooling and the maintenance of the NWP AAC (Wang et al., 2000). On its northwest flank, the anomalous southwesterly wind acts to strengthen the climatological southwesterly wind in the eastern Indochina Peninsula and southern China (Fig. 5a). This provides a potential dynamic condition for aerosol transport from the Indochina Peninsula to the downstream regions. Therefore, significant, positive AOD anomalies are observed over southern China (Fig. 4a). This is consistent with the findings of Zhao et al. (2018), which suggested that the transport of aerosols from South and Southeast Asia to southern China was enhanced during El Niño winters. Meanwhile, positive SSTAs appear over the entire tropical Indian Ocean, which is caused by El Niño (Xie et al., 2009). Accordingly, the tropical Indian Ocean sees northeasterly (northwesterly) wind anomalies near the surface to the north (south) of the equator. The anomalous northeasterly helps sustain the northern Indian Ocean warming (Du et al., 2009), which is also conducive to the maintaining of the NWP AAC (Xie et al., 2009, 2016). Conversely, the cold phase of ENSO (Fig. 5b) sees roughly opposite circulation anomaly pattern, with an anomalous cyclone over the NWP. Thus, the climatological southwesterly wind is weakened, suppressing aerosol transport from Southeast Asia to southern China. This may explain the AOD reduction in southern China (Fig. 4b). The differences between these two phases show similar anomalies to the warm phase but with a larger magnitude (Fig. 5c).

In addition to dynamic processes, the interannual aerosol variation may also be closely related to water vapour condition. For example, precipitation has a substantial effect on aerosol removal (e.g., Bao et al., 2009; Sanap and Pandithurai, 2015). It is shown that precipitation is largely suppressed over the western tropical Pacific (including the Indochina Peninsula) during the El Niño ensuing spring (Fig. 5a). However, because of the enhanced water vapour transportation by the NWP AAC (Zhang et al., 1999), precipitation is significantly increased in southern China and the south of Japan, where the AOD values are above normal (Fig. 3a). This indicates the aerosol transport could overwhelm the effect of precipitation (Zhang et al.,

https://doi.org/10.5194/acp-2020-859
Preprint. Discussion started: 29 October 2020


Atmospheric Chemistry and Physics Discussions

2010a; Zhao et al., 2018), which is consistent with the finding of Feng et al. (2017), which reported that the role of wet deposition was observed to be limited during the ENSO events.

According to the above analysis, the ENSO acts to modulate East Asian aerosols during the following spring mainly by changing the long-range transport of aerosols from Southeast Asia to the downstream region through the anomalous southwesterly wind on the northwest flank of the NWP AAC. Presumably, the Indochina Peninsula is the main source of East Asian spring aerosols. In the climatological mean state, the biomass burning in the Indochina Peninsula produces heavy smog and haze aerosol pollution during the dry season (February-April), especially in the valley of the northern Indochina Peninsula (Kim Oanh and Leelasakultum, 2011). The biomass burning-induced aerosols peak in March (Huang et al., 2016) and largely diminish after the monsoon onset in late April. During the dry season, the increasing aerosols can also affect the air quality in the downwind regions (Huang et al., 2016; Yadav et al., 2017; Zhang et al., 2018). It was reported that BC was the dominant emissions-driving factor, explaining 27.7 % of the AOD variance over Southeast Asia (Che et al., 2019).

Moreover, studies have shown that the ENSO can modulate biomass burning activities over the northern Indochina Peninsula in spring (e.g., Sanap and Pandithurai, 2015; Huang et al., 2016). Huang et al. (2016) suggested that the ENSO signal in the preceding winter strengthens the India-Burma Trough via the South China Sea anticyclone. This would provide drier airmass transported into the northern Indochina and thus promote local biomass burning activities. On the other hand, the aerosols generated by biomass burning could be affected by precipitation through the rainout and washout processes (Sanap and Pandithurai, 2015). CA (including both BC and OC) is the main by-product emitted from biomass burning and wildfire activities, which is usually used as a tracer to diagnose aerosol transport. As shown in Fig. 6, the anomalous AOD for CA is highly correlated to that for the total AOD during the ENSO ensuing spring, in terms of both spatial pattern and magnitude. This indicates that the aerosol anomalies are mainly contributed by CA, especially for La Niña events in which this contribution is nearly 100% (Fig. 6b). The spatial distribution of anomalies in horizontal CA flux and its divergence further confirm that the ENSO can modulate the emission and transportation of CA over East Asia. During the El Niño ensuing spring, abundant CA anomalies are transported to southern China, the East China Sea and the Kuroshio extension region from the Indochina Peninsula, with strong divergence over the northern Indochina Peninsula and convergence over southern China (Fig. 6a), while the opposite is detected for the La Niña ensuing spring (Fig. 6b).

From the temporal perspective, it is obvious that the mechanisms associated with ENSO's effects on East Asian aerosols are significantly different between spring and winter. Figure 7 shows the latitude-time cross sections of composite anomalies in total AOD, AOD of CA, and 850-hPa wind averaged along 100°–120°E for ENSO events. During the early winter [November(-1) to December(-1)] of the El Niño events, because El Niño-induced southeasterly anomalies act to weaken the EAWM, the AOD is increased over northern China between 35°and 45°N (Fig. 7a) mainly due to the suppressed local aerosol diffusion (Sun et al., 2018), while in the ensuing spring [MAM(0)], the significant, positive AOD anomalies appear south of 30°N, as persistent anomalous southwesterly wind provides a favourable dynamic condition for aerosol transport. In other words, the ENSO mainly affects the diffusion process of the local aerosols over northern China in winter, while it affects the long-range transport process of aerosols from the Indochina Peninsula to downstream in the ensuing spring.

https://doi.org/10.5194/acp-2020-859
Preprint. Discussion started: 29 October 2020


Atmospheric Chemistry and Physics Discussions

Besides, CA is the dominant component of these transported aerosols in spring [MAM(0)], especially in early spring [MA(0)], because El Niño-induced, suppressed precipitation in the northern Indochina Peninsula acts to promote the CA emission. The anomalous CA contributes more than 60% and 80% to the total AOD anomalies over the northern Indochina Peninsula and the South China in El Niño and La Niña spring, respectively (Fig. 7a-b).

As shown earlier, positive precipitation anomalies are observed over the downstream areas of aerosol transport during the El Niño ensuing spring, i.e., southern China (Fig. 5a). It is reported that increased remote transport and uplifting above clouds by the deep convection would increase the mid-to-upper tropospheric CA loading, even though the low-level CA is simultaneously removed by the strong precipitation washout effect (Lau et al., 2018). Thus, the meridional cross-sections of spring CA mixing ratio along 110°–125°E are examined next (Figs. 8a-c). Larger CA anomalies are located around 700hPa above the northern Indochina Peninsula (15°–25°N), which is a main pathway of CA transport from Southeast Asia to southern China by the westerlies (e.g., Lin et al., 2009; Zhou et al., 2018). During the El Niño (La Niña) ensuing spring (Figs. 8a-b), the enhanced (weakened) ascending motion is located to the north of 20°N, which corresponds to the enhanced (reduced) precipitation over southern China (Figs. 5a-b) and the increased (decreased) CA loading there from the surface to 150 hPa. This indicates that the CA mass can be lifted into the mid-upper troposphere by the enhanced vertical motion during the El Niño ensuing spring, which is then diffused over the downstream regions by the upper-level jet stream over the North Pacific (Fig. 8d) and causes changes in extratropical atmospheric circulation due to BC absorption (Shen and Ming, 2018).

5 Different influences of the two types of ENSO

In recent decades, a number of studies demonstrated that the impacts of CP ENSO on the East Asian climate are distinct from those of EP ENSO (e.g., Ashok et al., 2007; Weng et al., 2009; Feng and Li, 2011; Feng et al., 2011). What are the different influences of the two types of ENSO on ensuing spring aerosols over East Asia? Figure 9 shows composite spring AOD anomalies associated with EP and CP ENSO events, respectively. The AOD anomaly pattern during EP ENSO is similar to that during the ENSO (Fig. 4), except with much larger magnitude. During the EP El Niño ensuing spring (Fig. 9a), the positive AOD anomaly centre exceeds 0.12 over the northeastern and central Indochina Peninsula, while the largest negative anomaly is approximately -0.12 during the EP La Niña ensuing spring (Fig. 9c). Thus, asymmetric effects are still obvious. The area coverage with significant positive AOD anomalies during the EP ENSO is approximately as wide as that during the ENSO (Fig. 9e).

Compared with ENSO, the CP ENSO produces much smaller AOD anomalies (Figs. 9b, d, f). During the CP El Niño, positive anomalies occur over a band from the Indochina Peninsula across southern China to the Kuroshio extension (Fig. 9b), while the opposite is seen during the CP La Niña, with negative but insignificant AOD anomalies over the Indochina Peninsula and southern China (Figs. 9d, f). This means the AOD anomalies in this region are unstable.

https://doi.org/10.5194/acp-2020-859
Preprint. Discussion started: 29 October 2020


Atmospheric Chemistry and Physics Discussions

Clearly, as more typical, conventional ENSO events, the EP ENSO tends to cause larger positive AOD anomalies over the Indochina Peninsula and southern China in spring, while the CP ENSO causes smaller and statistically insignificant AOD anomalies. The atmospheric circulation anomalies of the two types of ENSO can explain this phenomenon. For the EP ENSO (Figs. 10a, c, e), the SSTAs exhibit a dipole pattern in the equatorial Pacific, which provides a favourable dynamic condition for aerosol transport through triggering the NWP AAC; while the CP ENSO is associated with a tripolar SST anomaly pattern (Ashok et al., 2007; also in Fig. 10b) and the AAC only occurs over southern China (Feng and Li, 2011). The anomalous southwesterly wind from the Indochina Peninsula to southern China is insignificant (Fig. 10f), likely resulting in the varying AOD anomalies (Fig. 9f).

To further investigate the relationship between spring East Asia aerosols and CP ENSO, Figure 11 shows the scatter plot between standardized AOD_IA and preceding winter Niño3.4 indices for all ENSO events. Overall, the EP El Niño (La Niña) events are associated with increasing (decreasing) AOD during the ensuing spring, indicative of a robust relationship between the two. However, no consistent relationships are found between AOD and CP ENSO events. For example, three CP El Niño events (2004/05, 2006/07 and 2009/10) correspond to higher AOD index, while two events (1994/95 and 2002/03) are associated with lower AOD index. In other words, these CP ENSO events can be divided into two groups: one associated with increasing AOD and the other associated with decreasing AOD during the ensuing spring. This is consistent with the previous studies (Feng et al., 2016a, 2017). Therefore, to better understand the impacts of CP ENSO on the springtime aerosols over East Asia, further investigations is needed on the basis of two different groups of CP ENSO events in future study.

6 Conclusions and discussion

In this study, we investigate the effects of ENSO on the ensuing spring aerosols over East Asia based on the NASA MERRA-2 aerosol reanalysis data during 1980–2019; we also discuss different effects of the two ENSO types. The East Asian AOD shows strong interannual variability in spring, which is coherently correlated with the SSTAs in the equatorial Pacific and Indian Ocean from the preceding autumn to concurrent spring. This implies that the interannual variability of East Asian spring aerosols may be modulated by the ENSO. Results from composite analyses reveal that the above-normal (below-normal) aerosols are found over the south of Japan, southern China, Indochina Peninsula and northern equatorial Maritime Continent during the El Niño (La Niña) ensuing spring. An obvious asymmetry is found in the AOD responses to the ENSO between the cold and warm phases.

During the ensuing spring, CA largely contribute to the interannual variability of East Asian aerosols, generally exceeding 60% for El Niño and exceeding 80% for La Niña. The associated atmospheric conditions show that over the source region of the northern Indochina Peninsula, the drier air, due to the enhanced India-Burma Trough and less precipitation, acts to increase biomass burning activities that emit more CA during the El Niño ensuing spring (Huang et al., 2016). On the other hand, the low-level southwesterly wind from the northern Indochina Peninsula across southern China to southern Japan is

https://doi.org/10.5194/acp-2020-859
Preprint. Discussion started: 29 October 2020


Atmospheric Chemistry and Physics Discussions

strengthened by the NWP AAC associated with El Niño, which acts to transport aerosols to the downstream regions. This is quite different from the modulation of interannual aerosol variability by the ENSO in winter through influencing local diffusion. Meanwhile, anomalous precipitation only reduces the aerosols over the source region, and its washout effect is limited over the downstream regions. This is likely because the amount of aerosols transported into these regions is much larger than that removed by precipitation, resulting in a net positive effect. Furthermore, the AOD anomaly patterns for both types of ENSO are similar to that of the ENSO, except for larger anomalies in the EP ENSO and smaller, insignificant anomalies in the CP ENSO because both AOD surplus and deficit can be seen during the warm phase of CP ENSO.

Note that the significant effects of ENSO on the ensuing spring aerosols are only confined to some regions of East Asia, i.e. southern China and the Indochina Peninsula. However, the AOD anomalies over other regions, such as northern China, are unstable, which is likely due to the coordinated influence of other climate systems, such as the Arctic Oscillation (Zhang et al., 2019) and North Atlantic Oscillation (Feng et al., 2019). Here, we only focus on the ENSO signal in the aerosols and do not take into account of other climate signals. Additionally, certain uncertainty might exist in the data due to the limitation of the MERRA-2 aerosol species concentrations for interannual variability analysis. The changes of aerosol composition in the MERRA-2 system are simulated by the widely-used chemical model of the Goddard Chemistry Aerosol Radiation and Transport (GOCART), and then the system adjusts the model simulation based on the total AOD retrieved from satellite measurements during assimilation, without directly considering the speciated aerosol information obtained from the satellite data. This may introduce artefacts for the increase or decrease of individual aerosol mass or AOD (Chin et al., 2002). Besides, the aerosol species emission inventories for the MERRA-2 have not been updated since the mid-2000s (Randles et al., 2017). These may also introduce some uncertainties in our analyses.

In addition, Lau et al. (2006) suggested that absorbing aerosols may lead to an advance of the rainy period and subsequently an intensification of the Indian summer monsoon (i.e., the “elevated heat pump” effect), thus amplifying the Indian summer monsoon response to ENSO forcing (Kim et al., 2016). As mentioned above, during the decaying spring of EP El Niño year, a large amount of absorbing aerosols produced in the source region (northern Indochina Peninsula) is transported to the downstream regions and even lifted up into the mid and upper troposphere, and then diffused to the North Pacific along with the westerly jets. Therefore, it would be interesting to explore the effects of absorbing aerosols on weather patterns or climate systems, including extratropical cyclones, North Pacific storm track and the EASM.

Data availability.

The ERA-5 Reanalysis data are available at https://cds.climate.copernicus.eu/cdsapp#!/search?type=dataset. MERRA-2 aerosol reanalysis data are available at https://disc.gsfc.nasa.gov/datasets. The CMAP precipitation data are available at www.esrl.noaa.gov/psd/, and the SST data of Met Office Hadley Centre are available at https://www.metoffice.gov.uk/hadobs/hadisst/.

https://doi.org/10.5194/acp-2020-859
Preprint. Discussion started: 29 October 2020

Atmospheric Chemistry and Physics Discussions

Author contributions.

HX and AZ designed the research. AZ performed the data analysis. SL contributed to the MERRA-2 data retrieval. HX, JD, and JM provided advice from the analysis perspective and all authors wrote the manuscript.

Acknowledgments

This work is jointly supported by the National Natural Science Foundation of China (41975106, 41705054, and 41805051). J. Deng is also supported by the Natural Science Foundation of Jiangsu Province (BK20170942). J. Ma is supported by the Startup Foundation for Introducing Talent of NUIST (2017r057). The numerical calculations in this paper have been done on the high performance computing system in the High Performance Computing Center, Nanjing University of Information Science & Technology.

Competing interests.

The authors declare that they have no conflict of interest.

https://doi.org/10.5194/acp-2020-859
Preprint. Discussion started: 29 October 2020

Atmospheric Chemistry and Physics Discussions

References

Allen, R. J., Sherwood, S. C., Norris, J. R., and Zender, C. S.: Recent Northern Hemisphere tropical expansion primarily driven by black carbon and tropospheric ozone, Nature, 485, 350, 10.1038/nature11097, 2012.

An, Z., Huang, R.-J., Zhang, R., Tie, X., Li, G., Cao, J., Zhou, W., Shi, Z., Han, Y., Gu, Z., and Ji, Y.: Severe haze in northern China: A synergy of anthropogenic emissions and atmospheric processes, P. Natl. Acad. Sci. USA, 116, 8657-8666, 10.1073/pnas.1900125116, 2019.

Ashok, K., Behera, S. K., Rao, S. A., Weng, H., and Yamagata, T.: El Niño Modoki and its possible teleconnection, J. Geophys. Res.-Oceans, 112, 10.1029/2006jc003798, 2007.

Awan, J. A., and Bae, D.-H.: Features and interdecadal variability of droughts in the homogeneous rainfall zones over the East Asian monsoon region, Int. J. Climatol., 36, 1943-1953, 10.1002/joc.4471, 2016.

Bao, Z., Wen, Z., and Wu, R.: Variability of aerosol optical depth over east Asia and its possible impacts, J. Geophys. Res.-Atmos., 114, 10.1029/2008jd010603, 2009.

Buchard, V., Randles, C. A., Silva, A. M. d., Darmenov, A., Colarco, P. R., Govindaraju, R., Ferrare, R., Hair, J., Beyersdorf, A. J., Ziemba, L. D., and Yu, H.: The MERRA-2 aerosol reanalysis, 1980 onward. Part II: Evaluation and case studies, J. Climate, 30, 6851-6872, 10.1175/jcli-d-16-0613.1, 2017.

Chan, C. K., and Yao, X.: Air pollution in mega cities in China, Atmos. Environ., 42, 1-42, https://doi.org/10.1016/j.atmosenv.2007.09.003, 2008.

Che, H., Gui, K., Xia, X., Wang, Y., Holben, B. N., Goloub, P., Cuevas-Agulló, E., Wang, H., Zheng, Y., Zhao, H., and Zhang, X.: Large contribution of meteorological factors to inter-decadal changes in regional aerosol optical depth, Atmos. Chem. Phys., 19, 10497-10523, 10.5194/acp-19-10497-2019, 2019.

Chin, M., Ginoux, P., Kinne, S., Torres, O., Holben, B. N., Duncan, B. N., Martin, R. V., Logan, J. A., Higurashi, A., and Nakajima, T.: Tropospheric aerosol optical thickness from the GOCART model and comparisons with satellite and Sun photometer measurements, J. Atmos. Sci., 59, 461-483, 10.1175/1520-0469(2002)059<0461:taotft>2.0.co;2, 2002.

Cohen, A. J., Brauer, M., Burnett, R., Anderson, H. R., Frostad, J., Estep, K., Balakrishnan, K., Brunekreef, B., Dandona, L., Dandona, R., Feigin, V., Freedman, G., Hubbell, B., Jobling, A., Kan, H., Knibbs, L., Liu, Y., Martin, R., Morawska, L., Pope, C. A., Shin, H., Straif, K., Shaddick, G., Thomas, M., van Dingenen, R., van Donkelaar, A., Vos, T., Murray, C. J. L., and Forouzanfar, M. H.: Estimates and 25-year trends of the global burden of disease attributable to ambient air pollution: an analysis of data from the Global Burden of Diseases Study 2015, The Lancet, 389, 1907-1918, https://doi.org/10.1016/S0140-6736(17)30505-6, 2017.

Deng, J., Dai, A., and Xu, H.: Nonlinear climate responses to increasing CO2 and anthropogenic aerosols simulated by CESM1, J. Climate, 33, 281-301, 10.1175/jcli-d-19-0195.1, 2020.

Du, Y., Xie, S.-P., Huang, G., and Hu, K.: Role of air-sea interaction in the long persistence of El Niño–induced north Indian Ocean warming, J. Climate, 22, 2023-2038, 10.1175/2008jcli2590.1, 2009.

https://doi.org/10.5194/acp-2020-859
Preprint. Discussion started: 29 October 2020

Feng, J., Chen, W., Tam, C.-Y., and Zhou, W.: Different impacts of El Niño and El Niño Modoki on China rainfall in the decaying phases, Int. J. Climatol., 31, 2091-2101, 10.1002/joc.2217, 2011.

Feng, J., and Li, J.: Influence of El Niño Modoki on spring rainfall over south China, J. Geophys. Res.-Atmos., 116, 10.1029/2010jd015160, 2011.

Feng, J., Li, J., Zhu, J., and Liao, H.: Influences of El Niño Modoki event 1994/1995 on aerosol concentrations over southern China, J. Geophys. Res.-Atmos., 121, 1637-1651, 10.1002/2015jd023659, 2016a.

Feng, J., Zhu, J., and Li, Y.: Influences of El Niño on aerosol concentrations over eastern China, Atmos. Sci. Lett., 17, 422-430, 10.1002/asl.674, 2016b.

Feng, J., Li, J., Zhu, J., Liao, H., and Yang, Y.: Simulated contrasting influences of two La Niña Modoki events on aerosol concentrations over eastern China, J. Geophys. Res.-Atmos., 122, 2734-2749, 10.1002/2016jd026175, 2017.

Feng, J., Li, J., Liao, H., and Zhu, J.: Simulated coordinated impacts of the previous autumn North Atlantic Oscillation (NAO) and winter El Niño on winter aerosol concentrations over eastern China, Atmos. Chem. Phys., 19, 10787-10800, 10.5194/acp-19-10787-2019, 2019.

Forster, P., Ramaswamy, V., Artaxo, P., Berntsen, T., Betts, R., Fahey, D. W., Haywood, J., Lean, J., Lowe, D. C., Myhre, G., Nganga, J., Prinn, R., Raga, G., Schultz, M., and Van Dorland, R.: Changes in atmospheric constituents and in radiative forcing, Cambridge University Press, Cambridge, United Kingdom, 129-234, 2007.

Gao, H., and Li, X.: Influences of El Nino Southern Oscillation events on haze frequency in eastern China during boreal winters, Int. J. Climatol., 35, 2682-2688, 10.1002/joc.4133, 2015.

Gelaro, R., McCarty, W., Suárez, M. J., Todling, R., Molod, A., Takacs, L., Randles, C. A., Darmenov, A., Bosilovich, M. G., Reichle, R., Wargan, K., Coy, L., Cullather, R., Draper, C., Akella, S., Buchard, V., Conaty, A., Silva, A. M. d., Gu, W., Kim, G.-K., Koster, R., Lucchesi, R., Merkova, D., Nielsen, J. E., Partyka, G., Pawson, S., Putman, W., Rienecker, M., Schubert, S. D., Sienkiewicz, M., and Zhao, B.: The modern-era retrospective analysis for research and applications, version 2 (MERRA-2), J. Climate, 30, 5419-5454, 10.1175/jcli-d-16-0758.1, 2017.

Gong, S. L., Zhang, X. Y., Zhao, T. L., Zhang, X. B., Barrie, L. A., McKendry, I. G., and Zhao, C. S.: A simulated climatology of Asian dust aerosol and its trans-Pacific transport. Part II: Interannual variability and climate connections, J. Climate, 19, 104-122, 10.1175/jcli3606.1, 2006.

Harrison, D. E., and Larkin, N. K.: The COADS sea level pressure signal: A near-global El Niño composite and time series view, 1946-1993, J. Climate, 9, 3025-3055, 10.1175/1520-0442(1996)009<3025:tcslps>2.0.co;2, 1996.

Heidinger, A. K., Foster, M. J., Walther, A., and Zhao, X.: The pathfinder atmospheres–extended AVHRR climate dataset, B. Am. Meteorol. Soc., 95, 909-922, 10.1175/bams-d-12-00246.1, 2014.

Hersbach, H., and Dee, D.: ERA5 reanalysis is in production, ECMWF newsletter, 147, 5-6, 2016.

Holben, B. N., Eck, T. F., Slutsker, I., Tanré, D., Buis, J. P., Setzer, A., Vermote, E., Reagan, J. A., Kaufman, Y. J., Nakajima, T., Lavenu, F., Jankowiak, I., and Smirnov, A.: AERONET—A federated instrument network and data archive for aerosol characterization, Remote. Sens. Environ., 66, 1-16, https://doi.org/10.1016/S0034-4257(98)00031-5, 1998.

https://doi.org/10.5194/acp-2020-859
Preprint. Discussion started: 29 October 2020

Huang, W.-R., Wang, S.-H., Yen, M.-C., Lin, N.-H., and Promchote, P.: Interannual variation of springtime biomass burning in Indochina: Regional differences, associated atmospheric dynamical changes, and downwind impacts, J. Geophys. Res.-Atmos., 121, 10,016-010,028, 10.1002/2016jd025286, 2016.

Kahn, R. A., Gaitley, B. J., Martonchik, J. V., Diner, D. J., Crean, K. A., and Holben, B.: Multiangle Imaging Spectroradiometer (MISR) global aerosol optical depth validation based on 2 years of coincident Aerosol Robotic Network (AERONET) observations, J. Geophys. Res.-Atmos., 110, 10.1029/2004jd004706, 2005.

Kim, M.-K., Lau, W. K. M., Kim, K.-M., Sang, J., Kim, Y.-H., and Lee, W.-S.: Amplification of ENSO effects on Indian summer monsoon by absorbing aerosols, Clim. Dynam., 46, 2657-2671, 10.1007/s00382-015-2722-y, 2016.

Kim Oanh, N. T., and Leelasakultum, K.: Analysis of meteorology and emission in haze episode prevalence over mountain-bounded region for early warning, Sci. Total Environ., 409, 2261-2271, https://doi.org/10.1016/j.scitotenv.2011.02.022, 2011.

Kim, S.-W., Yoon, S.-C., Kim, J., and Kim, S.-Y.: Seasonal and monthly variations of columnar aerosol optical properties over east Asia determined from multi-year MODIS, LIDAR, and AERONET Sun/sky radiometer measurements, Atmos. Environ., 41, 1634-1651, https://doi.org/10.1016/j.atmosenv.2006.10.044, 2007.

Lau, K. M., Kim, M. K., and Kim, K. M.: Asian summer monsoon anomalies induced by aerosol direct forcing: the role of the Tibetan Plateau, Clim. Dynam., 26, 855-864, 10.1007/s00382-006-0114-z, 2006.

Lau, W. K. M., Yuan, C., and Li, Z.: Origin, maintenance and variability of the Asian Tropopause Aerosol Layer (ATAL): the roles of monsoon dynamics, Sci. Rep., 8, 3960, 10.1038/s41598-018-22267-z, 2018.

Lelieveld, J., Klingmüller, K., Pozzer, A., Pöschl, U., Fnais, M., Daiber, A., and Münzel, T.: Cardiovascular disease burden from ambient air pollution in Europe reassessed using novel hazard ratio functions, Eur. Heart J., 40, 1590-1596, 10.1093/eurheartj/ehz135, 2019.

Levy, R. C., Remer, L. A., Kleidman, R. G., Mattoo, S., Ichoku, C., Kahn, R., and Eck, T. F.: Global evaluation of the Collection 5 MODIS dark-target aerosol products over land, Atmos. Chem. Phys., 10, 10399-10420, 10.5194/acp-10-10399-2010, 2010.

Li, Z., Niu, F., Fan, J., Liu, Y., Rosenfeld, D., and Ding, Y.: Long-term impacts of aerosols on the vertical development of clouds and precipitation, Nat. Geosci., 4, 888-894, 10.1038/ngeo1313, 2011.

Li, Z., Zhang, W., Stuecker, M. F., Xu, H., Jin, F.-F., and Liu, C.: Different effects of two ENSO types on Arctic surface temperature in boreal winter, J. Climate, 32, 4943-4961, 10.1175/jcli-d-18-0761.1, 2019.

Lin, C. Y., Hsu, H. m., Lee, Y. H., Kuo, C. H., Sheng, Y. F., and Chu, D. A.: A new transport mechanism of biomass burning from Indochina as identified by modeling studies, Atmos. Chem. Phys., 9, 7901-7911, 10.5194/acp-9-7901-2009, 2009.

Liu, Y., Liu, J., and Tao, S.: Interannual variability of summertime aerosol optical depth over East Asia during 2000–2011: a potential influence from El Niño Southern Oscillation, Environ. Res. Lett., 8, 044034, 10.1088/1748-9326/8/4/044034, 2013.

Myhre, G., Shindell, D., Bréon, F. M., Collins, W., Fuglestvedt, J., Huang, J., Koch, D., Lamarque, J. F., Lee, D., Mendoza, B., Nakajima, T., Robock, A., Stephens, G., Takemura, T., and Zhang, H.: Anthropogenic and natural radiative forcing, in: Climate Change 2013: The Physical Science Basis. Contribution of Working Group I to the Fifth Assessment Report of the Intergovernmental Panel on Climate Change, edited by: Stocker, T. F., Qin, D., Plattner, G. K., Tignor, M., Allen, S. K., Doschung, J., Nauels, A., Xia, Y., Bex, V., and Midgley, P. M., Cambridge University Press, Cambridge, UK, 659-740, 2013.

Ning, G., Wang, S., Yim, S. H. L., Li, J., Hu, Y., Shang, Z., Wang, J., and Wang, J.: Impact of low-pressure systems on winter heavy air pollution in the northwest Sichuan Basin, China, Atmos. Chem. Phys., 18, 13601–13615, https://doi.org/10.5194/acp-18-13601-2018, 2018.

Niu, F., Li, Z., Li, C., Lee, K.-H., and Wang, M.: Increase of wintertime fog in China: Potential impacts of weakening of the Eastern Asian monsoon circulation and increasing aerosol loading, J. Geophys. Res.-Atmos., 115, 10.1029/2009jd013484, 2010.

Randles, C. A., Silva, A. M. d., Buchard, V., Colarco, P. R., Darmenov, A., Govindaraju, R., Smirnov, A., Holben, B., Ferrare, R., Hair, J., Shinozuka, Y., and Flynn, C. J.: The MERRA-2 aerosol reanalysis, 1980 onward. Part I: System description and data assimilation evaluation, J. Climate, 30, 6823-6850, 10.1175/jcli-d-16-0609.1, 2017.

Rayner, N. A., Parker, D. E., Horton, E. B., Folland, C. K., Alexander, L. V., Rowell, D. P., Kent, E. C., and Kaplan, A.: Global analyses of sea surface temperature, sea ice, and night marine air temperature since the late nineteenth century, J. Geophys. Res.-Atmos., 108, 10.1029/2002jd002670, 2003.

Ren, H.-L., and Jin, F.-F.: Niño indices for two types of ENSO, Geophys. Res. Lett., 38, 10.1029/2010gl046031, 2011.

Rosenfeld, D.: Suppression of rain and snow by urban and industrial air pollution, Science, 287, 1793-1796, 2000.

Rosenfeld, D., Lohmann, U., Raga, G. B., O'Dowd, C. D., Kulmala, M., Fuzzi, S., Reissell, A., and Andreae, M. O.: Flood or drought: How do aerosols affect precipitation?, Science, 321, 1309-1313, 10.1126/science.1160606, 2008.

Sanap, S. D., and Pandithurai, G.: The effect of absorbing aerosols on Indian monsoon circulation and rainfall: A review, Atmos. Res., 164-165, 318-327, https://doi.org/10.1016/j.atmosres.2015.06.002, 2015.

Shen, Z., and Ming, Y.: The influence of aerosol absorption on the extratropical circulation, J. Climate, 31, 5961-5975, 10.1175/jcli-d-17-0839.1, 2018.

Song, Z., Fu, D., Zhang, X., Wu, Y., Xia, X., He, J., Han, X., Zhang, R., and Che, H.: Diurnal and seasonal variability of PM2.5 and AOD in North China plain: Comparison of MERRA-2 products and ground measurements, Atmos. Environ., 191, 70-78, https://doi.org/10.1016/j.atmosenv.2018.08.012, 2018.

Streets, D. G., and Waldhoff, S. T.: Present and future emissions of air pollutants in China: SO2, NOx, and CO, Atmos. Environ., 34, 363-374, https://doi.org/10.1016/S1352-2310(99)00167-3, 2000.

Sun, E., Xu, X., Che, H., Tang, Z., Gui, K., An, L., Lu, C., and Shi, G.: Variation in MERRA-2 aerosol optical depth and absorption aerosol optical depth over China from 1980 to 2017, J. Atmos. Sol-Terr. Phy., 186, 8-19, https://doi.org/10.1016/j.jastp.2019.01.019, 2019.

https://doi.org/10.5194/acp-2020-859
Preprint. Discussion started: 29 October 2020


Atmospheric Chemistry and Physics Discussions

Sun, J., Li, H., Zhang, W., Li, T., Zhao, W., Zuo, Z., Guo, S., Wu, D., and Fan, S.: Modulation of the ENSO on winter aerosol pollution in the Eastern Region of China, J. Geophys. Res.-Atmos., 123, 11,952-911,969, 10.1029/2018jd028534, 2018.

Tao, J., Zhang, L., Cao, J., and Zhang, R.: A review of current knowledge concerning PM2. 5 chemical composition, aerosol optical properties and their relationships across China, Atmos. Chem. Phys., 17, 9485-9518, 10.5194/acp-17-9485-2017, 2017.

Wang, B., Wu, R., and Fu, X.: Pacific–East Asian teleconnection: how does ENSO affect East Asian climate?, J. Climate, 13, 1517-1536, 10.1175/1520-0442(2000)013<1517:peathd>2.0.co;2, 2000.

Wang, H.-J., Chen, H.-P., and Liu, J.: Arctic sea ice decline intensified haze pollution in eastern China, Atmos. Oceanic Sci. Lett., 8, 1-9, 10.3878/AOSL20140081, 2015.

Wang, H., Xie, S.-P., Kosaka, Y., Liu, Q., and Du, Y.: Dynamics of Asian aummer monsoon response to anthropogenic aerosol forcing, J. Climate, 32, 843-858, 10.1175/jcli-d-18-0386.1, 2019a.

Wang, X., Zhong, S., Bian, X., and Yu, L.: Impact of 2015–2016 El Niño and 2017–2018 La Niña on PM2.5 concentrations across China, Atmos. Environ., 208, 61-73, https://doi.org/10.1016/j.atmosenv.2019.03.035, 2019b.

Weng, H., Behera, S. K., and Yamagata, T.: Anomalous winter climate conditions in the Pacific rim during recent El Niño Modoki and El Niño events, Clim. Dynam., 32, 663-674, 10.1007/s00382-008-0394-6, 2009.

Werdell, P. J., Behrenfeld, M. J., Bontempi, P. S., Boss, E., Cairns, B., Davis, G. T., Franz, B. A., Gliese, U. B., Gorman, E. T., and Hasekamp, O.: The plankton, aerosol, cloud, ocean ecosystem mission: status, science, advances, B. Am. Meteorol. Soc., 100, 1775-1794, 2019.

Wu, G., Li, Z., Fu, C., Zhang, X., Zhang, R., Zhang, R., Zhou, T., Li, J., Li, J., Zhou, D., Wu, L., Zhou, L., He, B., and Huang, R.: Advances in studying interactions between aerosols and monsoon in China, Sci. China Earth Sci., 59, 1-16, 10.1007/s11430-015-5198-z, 2016.

Xie, P., and Arkin, P. A.: Global precipitation: A 17-year monthly analysis based on gauge observations, satellite estimates, and numerical model outputs, B. Am. Meteorol. Soc., 78, 2539-2558, 1997.

Xie, S.-P., Hu, K., Hafner, J., Tokinaga, H., Du, Y., Huang, G., and Sampe, T.: Ocean capacitor effect on Indo–western Pacific climate during the summer following El Niño, J. Climate, 22, 730-747, 10.1175/2008jcli2544.1, 2009.

Xie, S.-P., Kosaka, Y., Du, Y., Hu, K., Chowdary, J. S., and Huang, G.: Indo-western Pacific Ocean capacitor and coherent climate anomalies in post-ENSO summer: A review, Adv. Atmos. Sci., 33, 411-432, 10.1007/s00376-015-5192-6, 2016.

Yadav, I. C., Linthoingambi Devi, N., Li, J., Syed, J. H., Zhang, G., and Watanabe, H.: Biomass burning in Indo-China Peninsula and its impacts on regional air quality and global climate change-a review, Environ. Pollut., 227, 414-427, https://doi.org/10.1016/j.envpol.2017.04.085, 2017.

Yin, Z., and Wang, H.: Role of atmospheric circulations in haze pollution in December 2016, Atmos. Chem. Phys., 17, 11673-11681, 10.5194/acp-17-11673-2017, 2017.

Yu, X., Wang, Z., Zhang, H., and Zhao, S.: Impacts of different types and intensities of El Niño events on winter aerosols over China, Sci. Total Environ., 655, 766-780, https://doi.org/10.1016/j.scitotenv.2018.11.090, 2019.

Yuan, C., Lau, W. K. M., Li, Z., and Cribb, M.: Relationship between Asian monsoon strength and transport of surface aerosols to the Asian Tropopause Aerosol Layer (ATAL): interannual variability and decadal changes, Atmos. Chem. Phys., 19, 1901-1913, 10.5194/acp-19-1901-2019, 2019.

Yue, X., Unger, N., Harper, K., Xia, X., Liao, H., Zhu, T., Xiao, J., Feng, Z., and Li, J.: Ozone and haze pollution weakens net primary productivity in China, Atmos. Chem. Phys., 17, 6073-6089, 10.5194/acp-17-6073-2017, 2017.

Zhang, G., Gao, Y., Cai, W., Leung, L. R., Wang, S., Zhao, B., Wang, M., Shan, H., Yao, X., and Gao, H.: Seesaw haze pollution in North China modulated by the sub-seasonal variability of atmospheric circulation, Atmos. Chem. Phys., 19, 565-576, 10.5194/acp-19-565-2019, 2019.

Zhang, L., Liao, H., and Li, J.: Impacts of Asian summer monsoon on seasonal and interannual variations of aerosols over eastern China, J. Geophys. Res.-Atmos., 115, 10.1029/2009jd012299, 2010a.

Zhang, L., Liao, H., and Li, J.: Impact of the Southeast Asian summer monsoon strength on the outflow of aerosols from South Asia, Ann. Geophys., 28, 10.5194/angeo-28-277-2010, 2010b.

Zhang, M., Wang, Y., Ma, Y., Wang, L., Gong, W., and Liu, B.: Spatial distribution and temporal variation of aerosol optical depth and radiative effect in South China and its adjacent area, Atmos. Environ., 188, 120-128, https://doi.org/10.1016/j.atmosenv.2018.06.028, 2018.

Zhang, R., Sumi, A., and Kimoto, M.: A diagnostic study of the impact of El Niño on the precipitation in China, Adv. Atmos. Sci., 16, 229-241, 10.1007/BF02973084, 1999.

Zhang, R., Li, G., Fan, J., Wu, D. L., and Molina, M. J.: Intensification of Pacific storm track linked to Asian pollution, P. Natl. Acad. Sci. USA, 104, 5295-5299, 10.1073/pnas.0700618104, 2007.

Zhang, W., Jin, F.-F., Li, J., and Ren, H.-L.: Contrasting impacts of two-type El Niño over the western North Pacific during boreal autumn, J. Meteorol. Soc. Jpn. Ser. II, 89, 563-569, 10.2151/jmsj.2011-510, 2011.

Zhang, X., Sun, J., Wang, Y., Li, W., ZHang, Q., Wang, W., Quan, J., Cao, G., Wang, J., Yang, Y., and Zhang, Y.: Factors contributing to haze and fog in China, Chin. Sci. Bull., 58, 1178, https://doi.org/10.1360/972013-150, 2013.

Zhao, S., Zhang, H., and Xie, B.: The effects of El Niño–Southern Oscillation on the winter haze pollution of China, Atmos. Chem. Phys., 18, 1863-1877, 10.5194/acp-18-1863-2018, 2018.

Zhou, D., Ding, K., Huang, X., Liu, L., Liu, Q., Xu, Z., Jiang, F., Fu, C., and Ding, A.: Transport, mixing and feedback of dust, biomass burning and anthropogenic pollutants in eastern Asia: a case study, Atmos. Chem. Phys., 18, 16345-16361, 10.5194/acp-18-16345-2018, 2018.

Zou, Y., Wang, Y., Zhang, Y., and Koo, J.-H.: Arctic sea ice, Eurasia snow, and extreme winter haze in China, Sci. Adv., 3, e1602751, 10.1126/sciadv.1602751, 2017.

https://doi.org/10.5194/acp-2020-859
Preprint. Discussion started: 29 October 2020

Atmospheric Chemistry and Physics Discussions

Table 1: Two types of ENSO events during 1980-2019

	Eastern Pacific (EP) type	Central Pacific (CP) type
El Niño	1982/1983, 1986/87, 1991/92, 1997/98, 2015/16, 2018/19	1994/95, 2002/03, 2004/05, 2006/07, 2009/10
La Niña	1984/85, 1995/96, 1999/2000, 2005/06, 2007/08, 2017/18	1983/84, 1988/89, 2008/09, 2010/11, 2011/12, 2016/17

https://doi.org/10.5194/acp-2020-859
Preprint. Discussion started: 29 October 2020

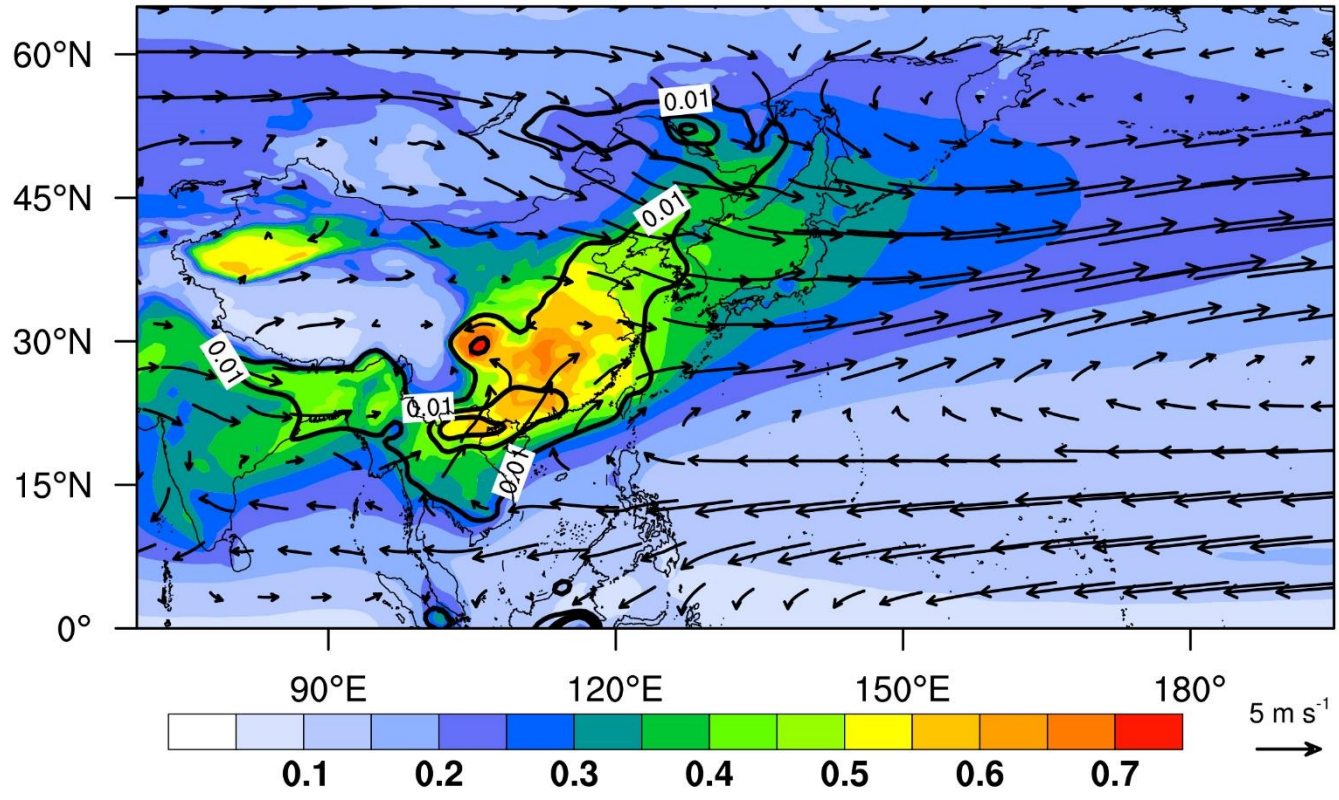

Figure 1: Spatital distirbution of climatological spring (MAM) mean aerosol optical depth (AOD; shading) and 850-hPa wind (vector; m s^{-1}). Black contours denote spring AOD's variance with interval of 0.02.

https://doi.org/10.5194/acp-2020-859
Preprint. Discussion started: 29 October 2020

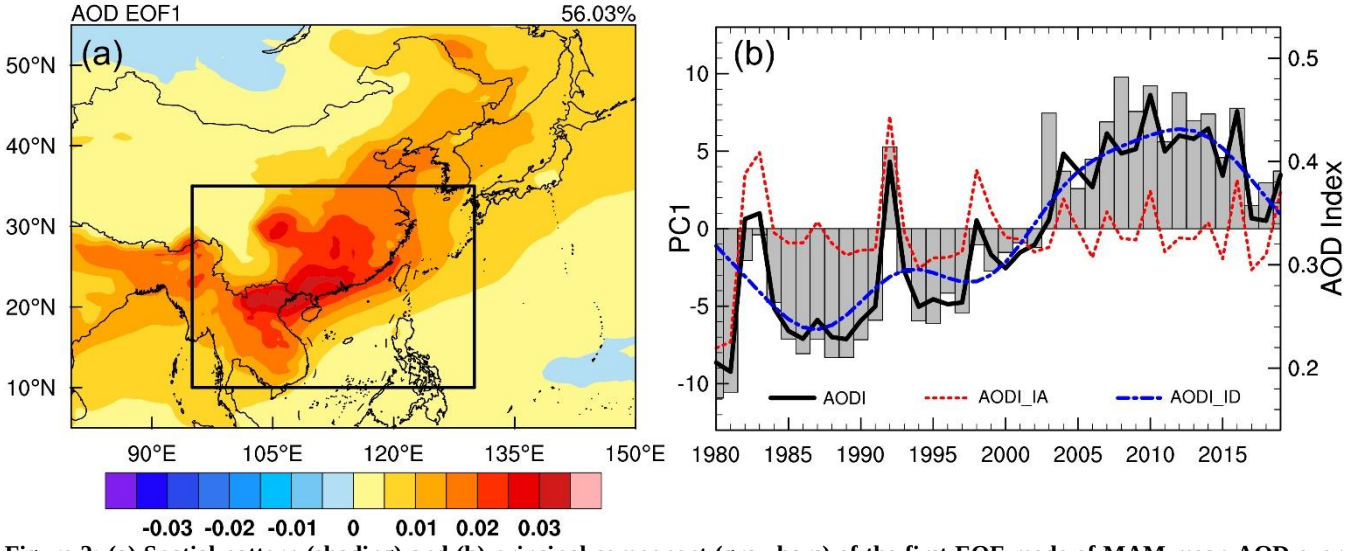

Figure 2: (a) Spatial pattern (shading) and (b) principal component (gray bars) of the first EOF mode of MAM mean AOD over East Asia during 1980–2019. The East Asian spring AOD index (AODI; black solid line) defined as AOD averaged over East Asia [95 °–130 °E, 10 °–35 °N; the black box in (a)] is also plotted in (b), together with its interannual component (AODI_IA; red dashed line) and interdecadal component (AODI_ID; blue dashed line).

https://doi.org/10.5194/acp-2020-859
Preprint. Discussion started: 29 October 2020

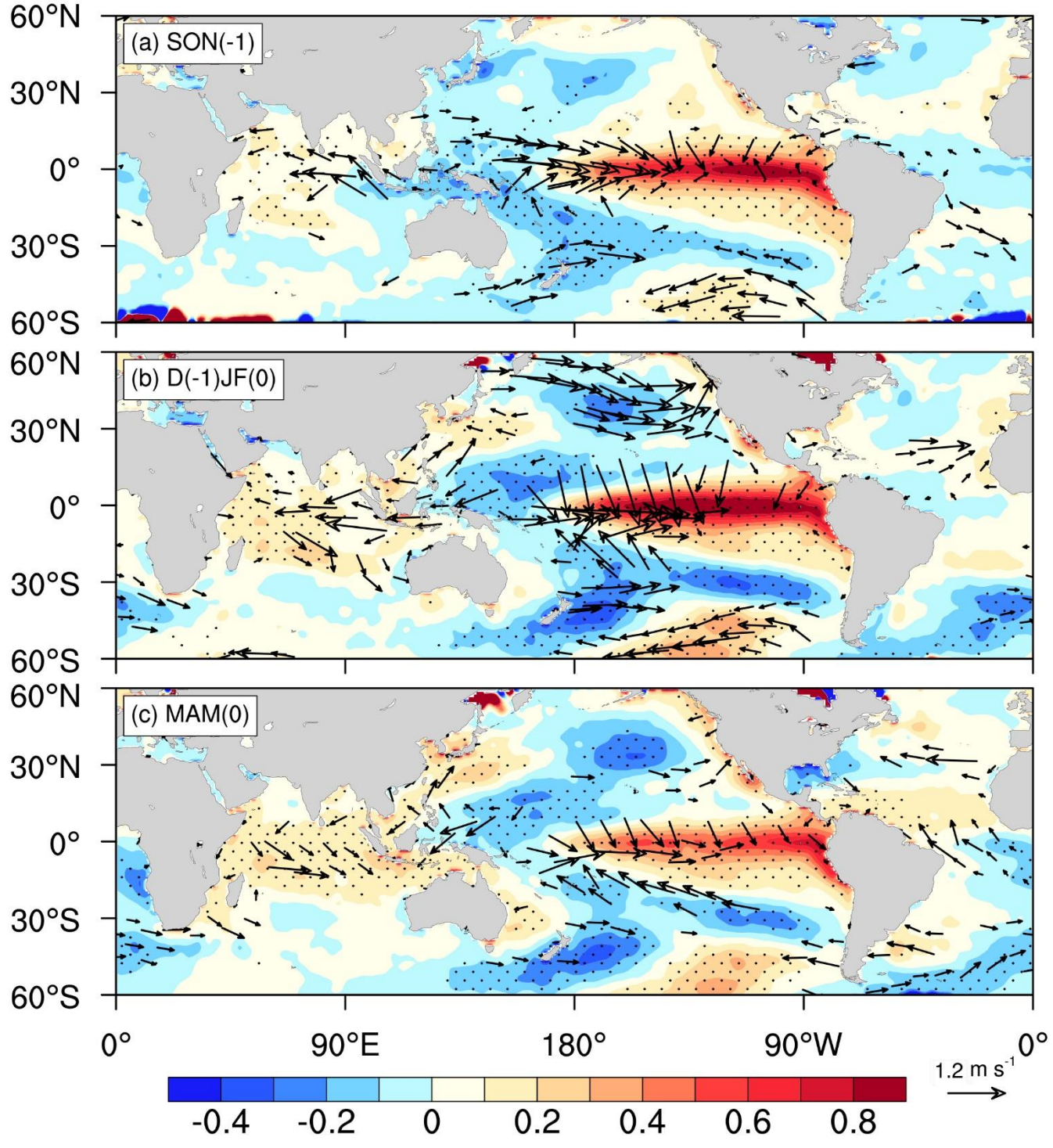

Figure 3: Regressions of sea surface temperature (SST) anomalies (shading; ℃) and 10-m surface wind anomalies (vector; m s^{-1}) onto the standardized AODI_IA in (a) preceding autumn [SON(-1)], (b) preceding winter [D(-1)JF(0)] and (c) simultaneous spring

https://doi.org/10.5194/acp-2020-859
Preprint. Discussion started: 29 October 2020

Atmospheric Chemistry and Physics Discussions

[MAM(0)]. Stippling and vector denote the regressed SST and wind are statistically significant at the 95% confidence level based on the Student's *t* test, respectively.

https://doi.org/10.5194/acp-2020-859
Preprint. Discussion started: 29 October 2020

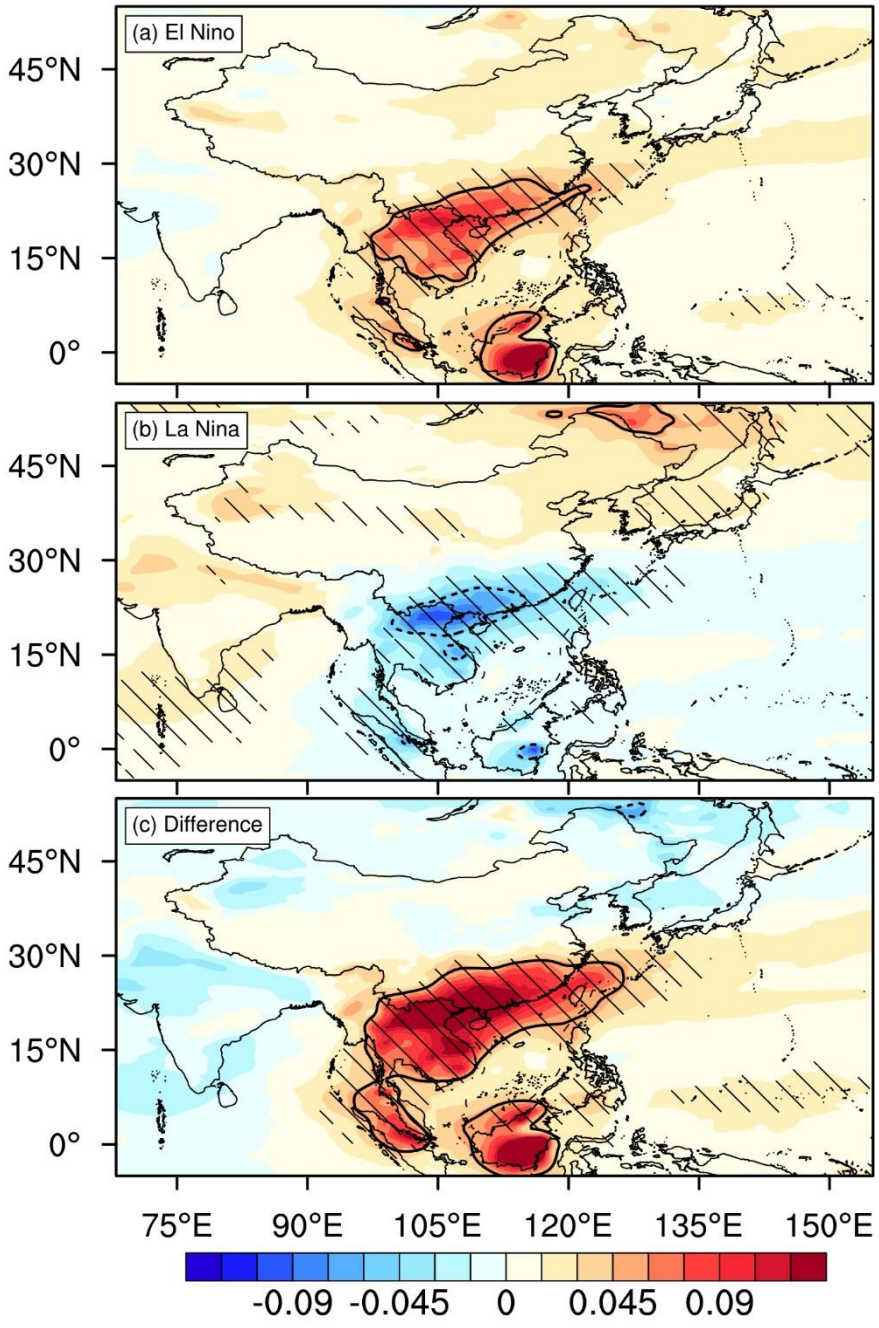

Figure 4: Composite anomalies of spring AOD (shading) during (a) El Niño, (b) La Niña and (c) their differences (El Niño minus La Niña). Black solid (dashed) contours outline the areas where the AOD anomalies are larger (smaller) than 0.05 (-0.05). Hatching denotes the anomalies statistically significant at the 95% confidence level based on the Student's *t* test.

https://doi.org/10.5194/acp-2020-859
Preprint. Discussion started: 29 October 2020

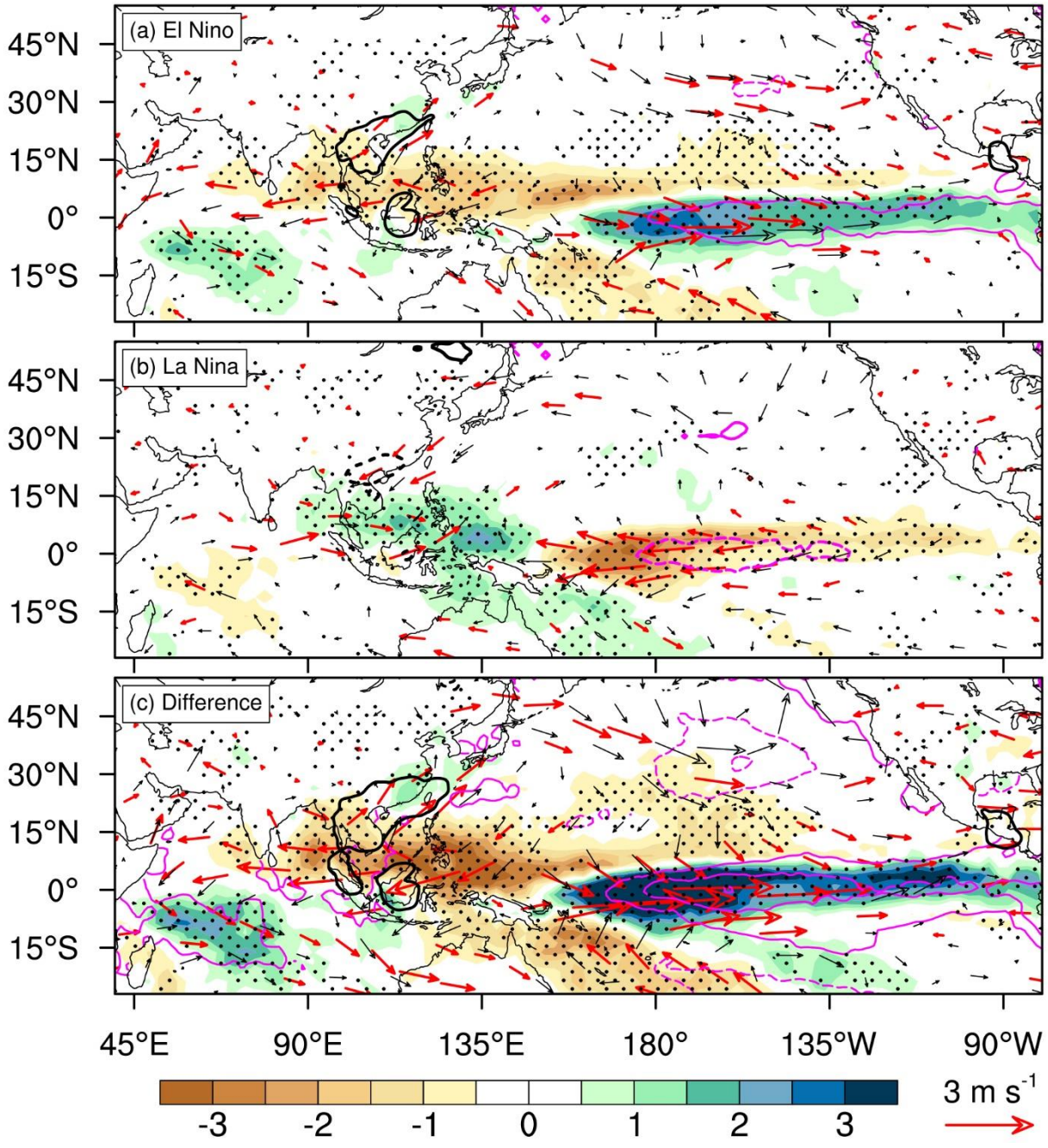

Figure 5: Same as Figure 4, except for SST anomalies (purple contours with interval of 0.05 ℃; the dashed contours are for negative values, and zero contour is omitted for clarity), precipitation anomalies (shading; mm day^{-1}) and 850-hPa wind anomalies (black vector; m s^{-1}). Black contours are the same as those in Figure 4. Stippling and red vector indicate the anomalies of precipitation and wind are statistically significant at the 95% confidence level based on the Student's *t* test, respectively.

https://doi.org/10.5194/acp-2020-859
Preprint. Discussion started: 29 October 2020

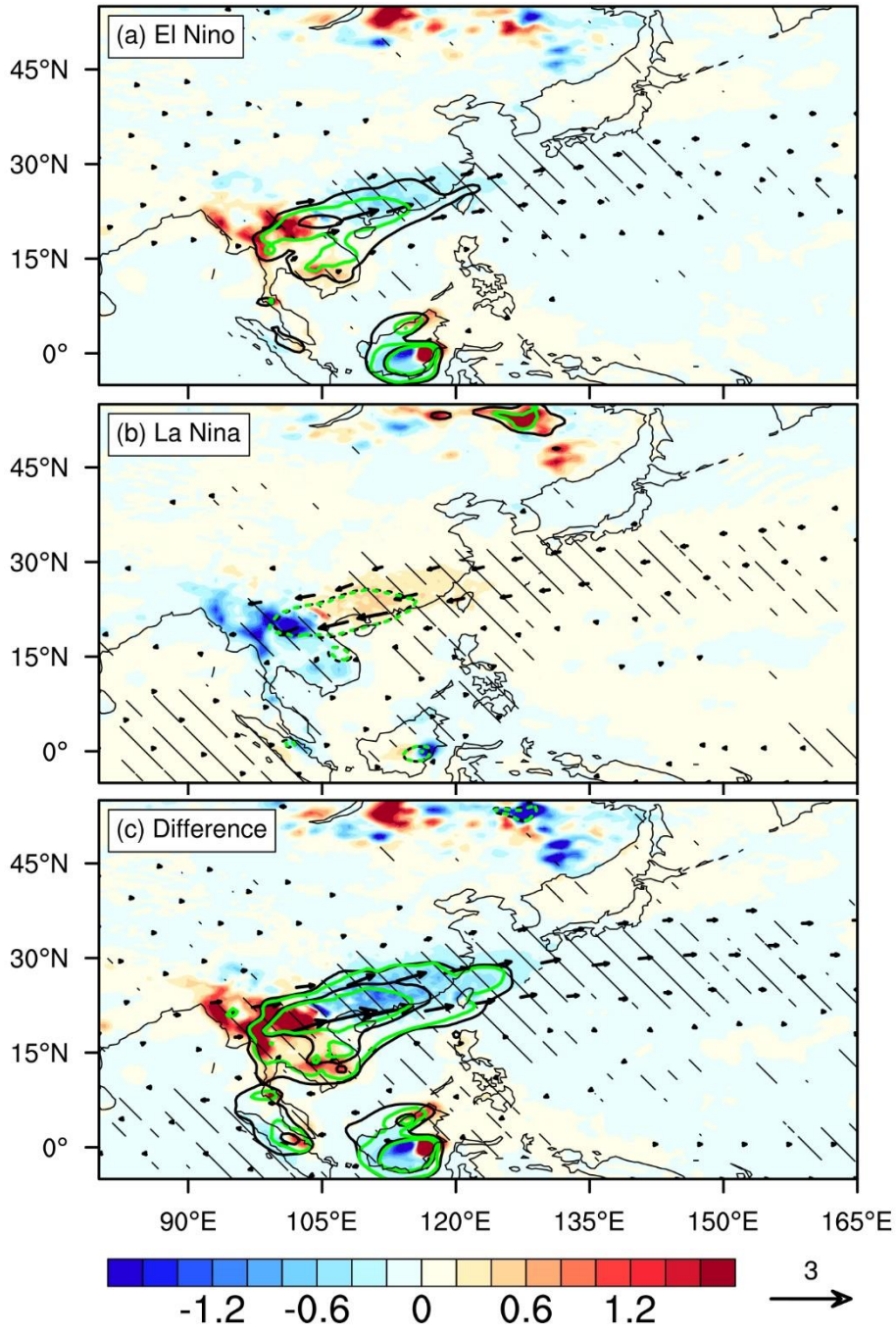

Figure 6: Composite anomalies of total AOD (black contour), AOD of carbonaceous aerosol (CA; green contours), CA flux (vector; 10^{-1} g m^{-1} s^{-1}) and its divergence (shading; 10^{-7} g m^{-2} s^{-1}) during (a) El Niño, (b) La Niña and (c) their difference (El Niño minus La Niña) in spring. The contour interval is 0.05; the dashed contours are for nagetive values, and the zero contour is omitted for clarity. Hatching and black vector represent the anomalies of CA flux and its divergence are statistically significant at the 95% confidence level based on the Student's *t* test, respectively.

https://doi.org/10.5194/acp-2020-859
Preprint. Discussion started: 29 October 2020

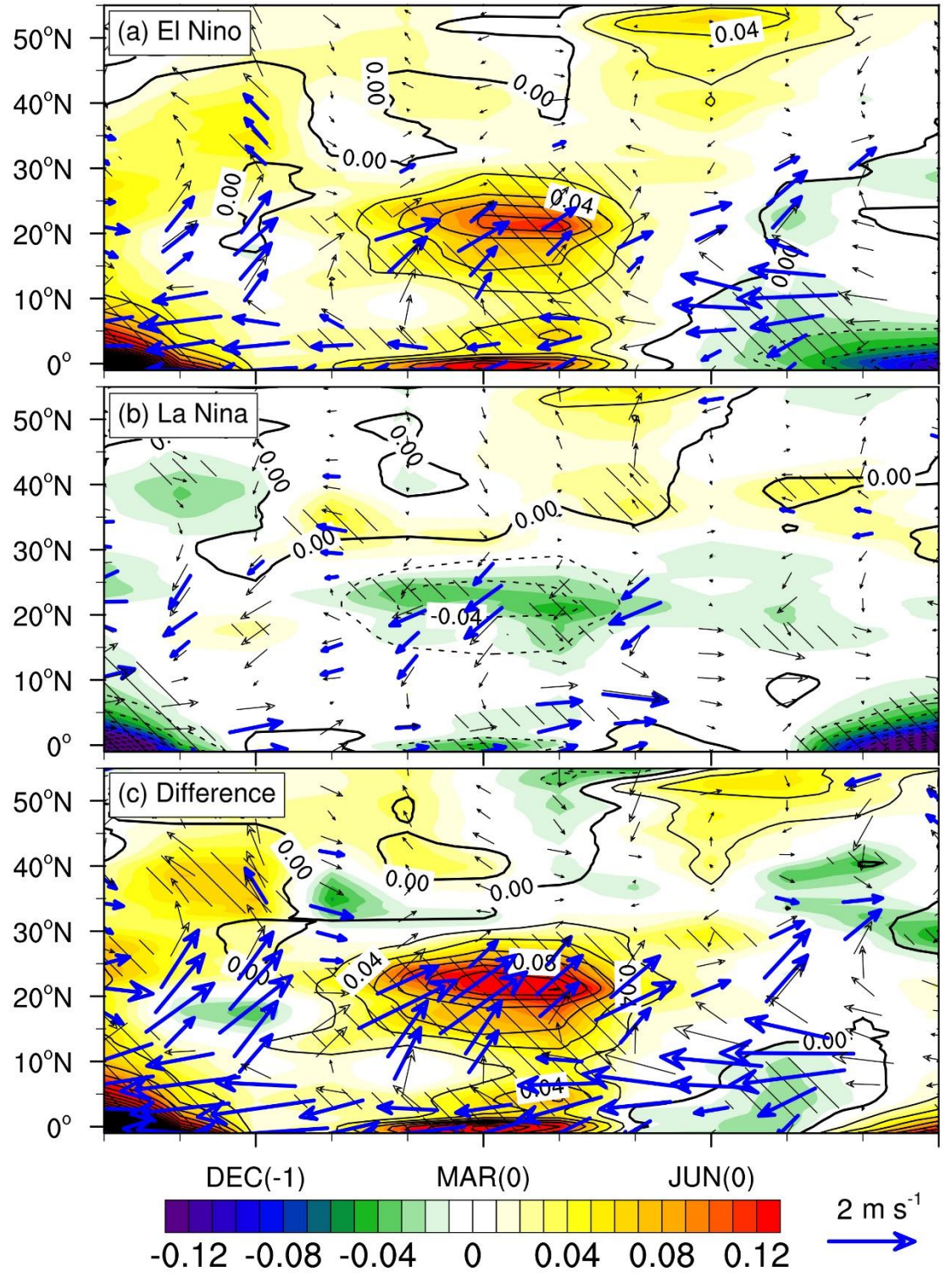

https://doi.org/10.5194/acp-2020-859
Preprint. Discussion started: 29 October 2020

Atmospheric Chemistry and Physics Discussions

Figure 7: Latitude-time cross sections of composite anomalies of AOD (shading), AOD of CA (black contour with interval of 0.02), and 850-hPa wind (vector; m s^{-1}) during (a) El Niño, (b) La Niña and (c) their difference (El Niño minus La Niña) averaged over 100 °–120 °E. Hatching and blue vector indicate the anomalies of AOD and winds are statistically significant at the 95% confidence level based on the Student's *t* test, respectively.

5

https://doi.org/10.5194/acp-2020-859
Preprint. Discussion started: 29 October 2020

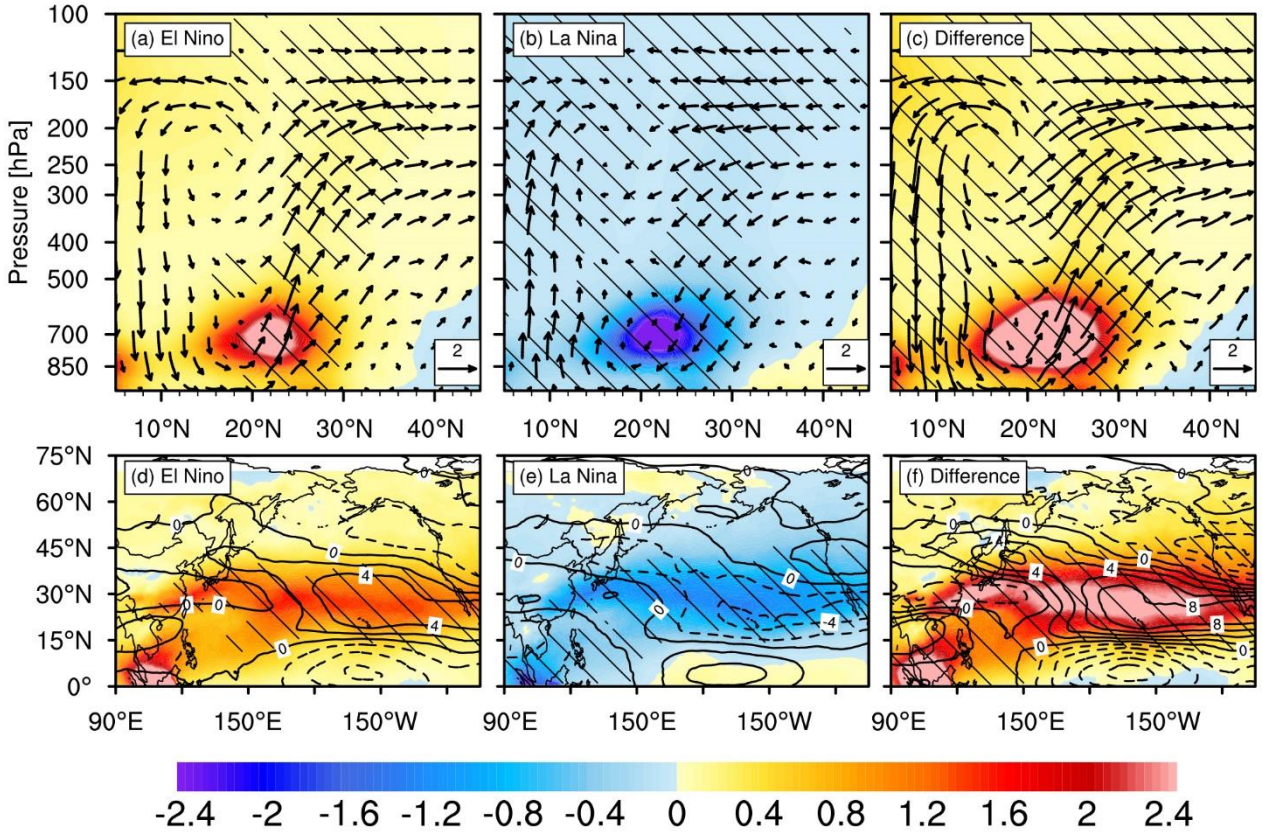

Figure 8: (a)-(c) Vertical sections of composite anomalies of spring CA mixing ratio (shading; 10^{-6} g kg^{-1}) and meridional and vertical velocities (vector; in m s^{-1} and 10^{-2} m s^{-1}, respectively) averaged over 105°–120°E during (a) El Niño (b) La Niña and (c) their difference (El Niño minus La Niña). (d)-(f) Same as Figure4, except for 300-hPa CA mixing ratio (shading; 10^{-7} g kg^{-1}) and zonal wind (contour with interval of 4 m s^{-1}). Hatching denotes the anomalies statistically significant at the 95% confidence level based on the Student's *t* test.

https://doi.org/10.5194/acp-2020-859
Preprint. Discussion started: 29 October 2020

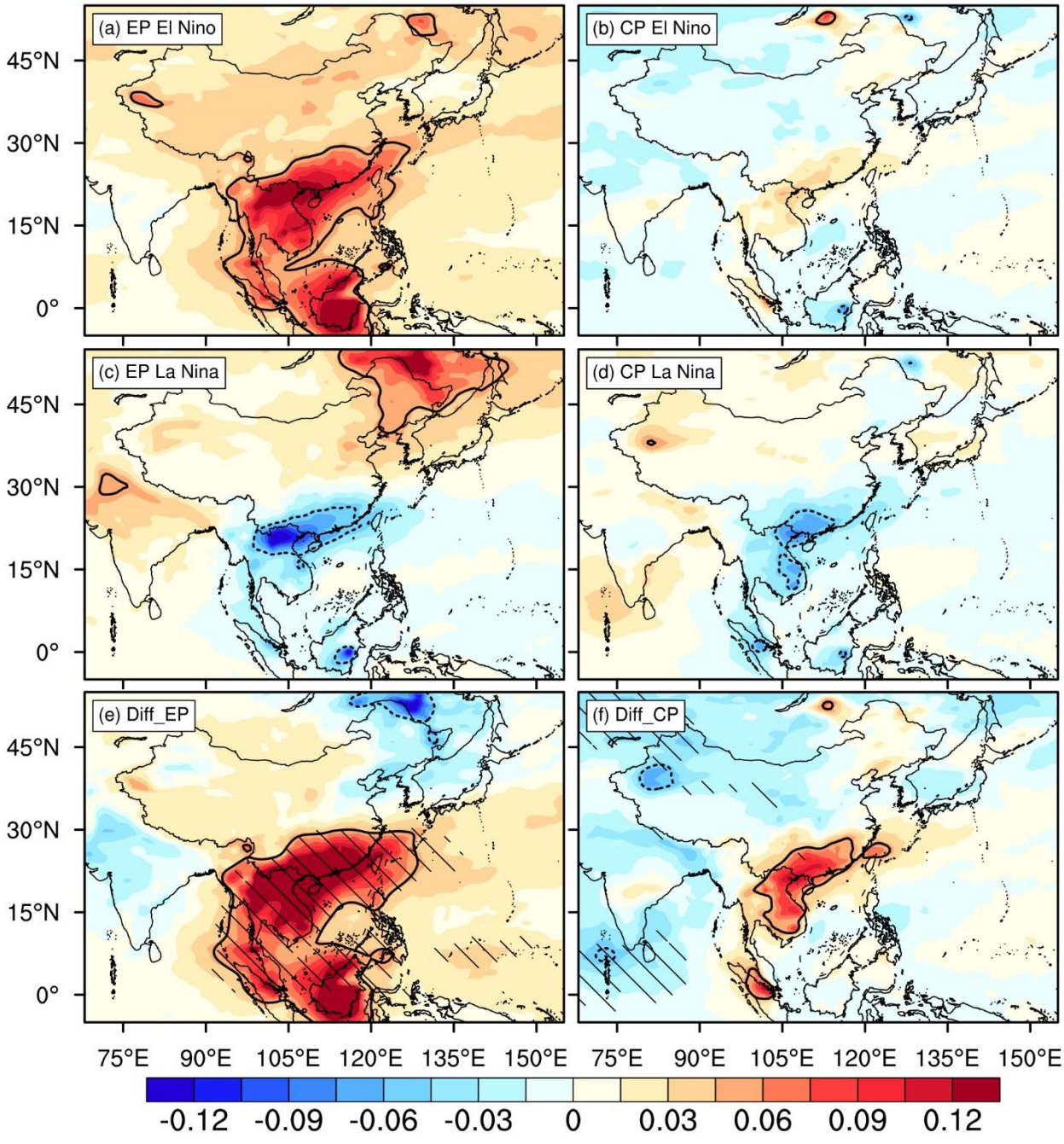

Figure 9: Same as Figure 4, except for (left) EP and (right) CP ENSO events.

https://doi.org/10.5194/acp-2020-859
Preprint. Discussion started: 29 October 2020

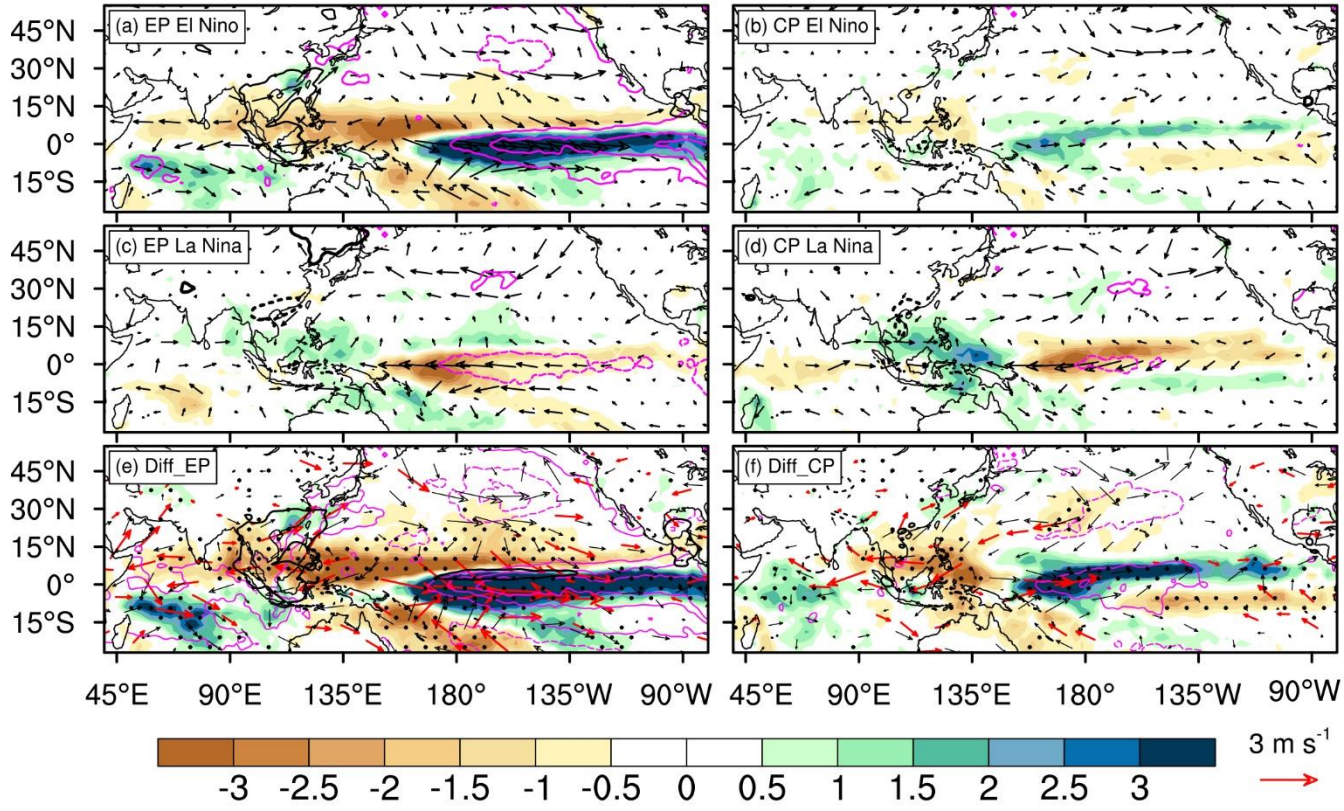

Figure 10: Same as Figure 5, except for (left) EP and (right) CP ENSO events.

https://doi.org/10.5194/acp-2020-859
Preprint. Discussion started: 29 October 2020

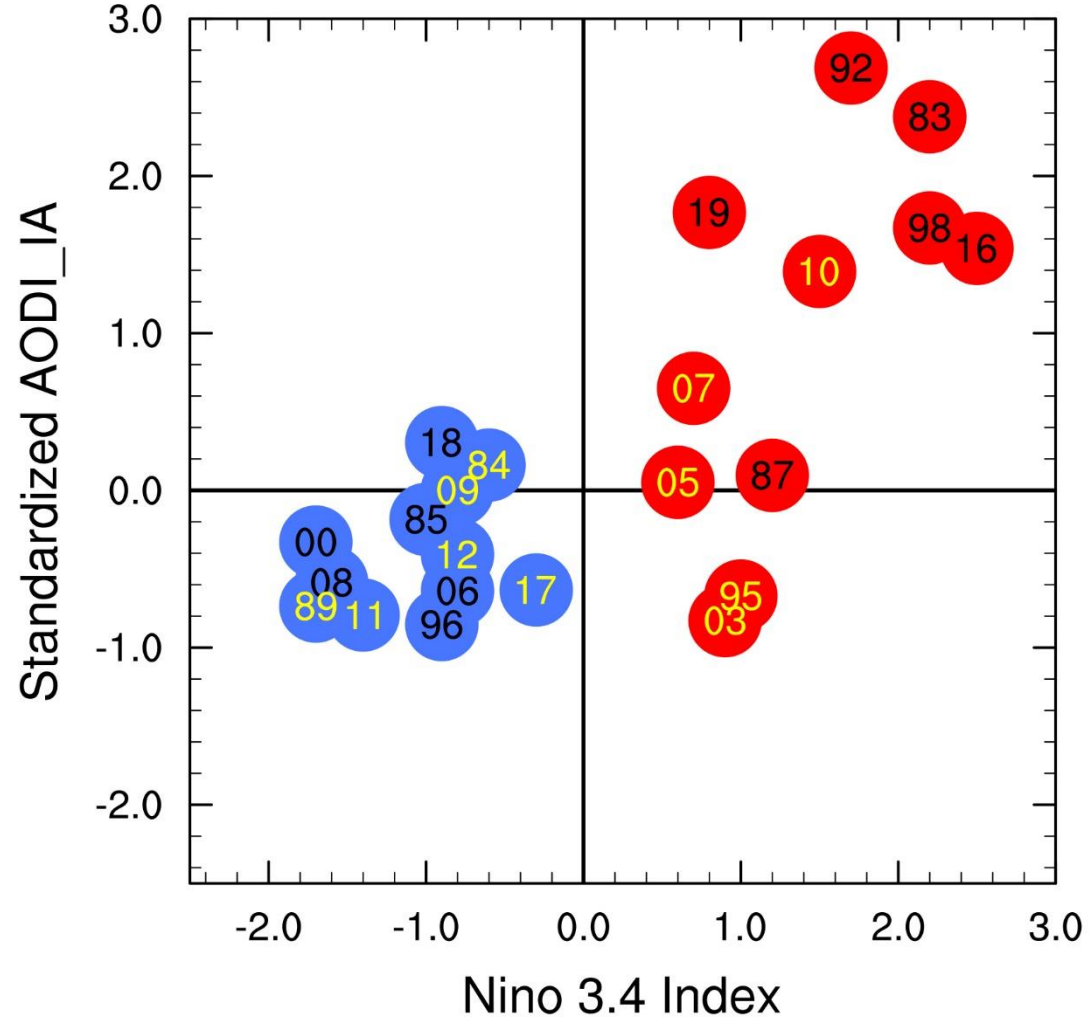

Figure 11: Scatter plot between standardized AODI_IA and corresponding preceding winter (DJF) Niño3.4 (℃) indices for 23 ENSO events. Eleven El Niño and twelve La Niña events are indicated by red and blue circles, respectively. The number inside each circle denotes the calendar year, with black and yellow for EP and CP ENSO, respectively.